

UNIVERSITY OF READING

MASTER'S DISSERTATION

Quantifying Long-Duration Storage Capacity and the Meteorological Drivers of Net-Zero Electricity Systems

Author:
Lainey WARD

Supervisors:
Dr. David BRAYSHAW
Dr. Hannah BLOOMFIELD
Ben HUTCHINS

*A thesis submitted in fulfillment of the requirements
for the degree of Atmosphere, Ocean and Climate*

in the
Department of Meteorology

August 11, 2024

UNIVERSITY OF READING

*Abstract***Quantifying Long-Duration Storage Capacity and the Meteorological Drivers of Net-Zero Electricity Systems**

by Lainey WARD

Achieving Net-Zero carbon emissions by 2050 is a critical goal for the UK, necessitating a transformative shift in its energy landscape. This study investigates the need for Long-Duration Storage (LDS) to address energy deficits under various Net-Zero pathways, focusing on axes of demand electrification and offshore wind power deployment. This study builds on existing literature by quantifying storage requirements within a historical context, using a 72-year ERA5-derived power dataset alongside an underground hydrogen storage model.

Initial storage capacity estimates for the chosen pathways are 88 TWh for Headwinds, 79 TWh for Balanced Pathway, and 49 TWh for Widespread Innovation. Accounting for uncertainties due to finite data series and projected changes in storage conversion efficiencies, these estimates rise to 123 TWh, 85 TWh, and 49 TWh, respectively. Findings suggest that scenarios with higher renewable energy deployment and extensive heating electrification require less LDS, while less advanced scenarios could require up to 2.5 times more capacity.

Meteorological drivers of LDS depletion are also explored, with a case study revealing that the most severe depletion event coincides with a high-pressure system over Scandinavia, reinforced by SST gradients, snow, and sudden stratospheric warming feedbacks.

Through K-means clustering, four key synoptic meteorological regimes were identified, with the Scandinavian-Iceland blocking regime requiring the highest storage capacity. This regime's infrequent but significant pan-European impact during periods of wind stilling highlights the need to account for future stilling in LDS deployment.

Composite analysis shows that high-renewable, high-electrification scenarios are driven by the same synoptic blocking systems as less advanced scenarios but require LDS only when wind speeds and temperatures fall below critical thresholds. A national UK analysis of power anomalies reveals that these scenarios are influenced by both wind and temperature, whereas low-electrification scenarios are driven primarily by wind.

While the study acknowledges limitations, it lays the groundwork for future research by combining an extended historical dataset with Net-Zero modelling to generate more robust LDS capacity estimates. These estimates are crucial for ensuring the resilience of a decarbonized UK electricity system amidst weather and climate variability into 2050 and beyond.

Acknowledgements

I would like to express my deepest gratitude to my supervisors, David, Hannah, and Ben, for their invaluable time and extensive research that laid the foundation for this dissertation. I also thank the Department of Meteorology for welcoming me into this degree programme, which has been an immensely rewarding experience.

This endeavour would not have been possible without the unwavering support of my friends, whose encouragement and companionship in the library were invaluable.

Contents

Abstract	ii
Acknowledgements	iii
1 Introduction	1
1.1 Motivation	2
1.2 Objectives	3
1.3 Outline	3
2 Literature Review	5
2.1 Flexibility	5
2.2 Net-Zero	6
2.2.1 Scenarios in the Literature	7
2.2.1 Consensus in the Literature	8
2.3 Quantifying Storage	9
2.3.1 LDS Principles	9
2.3.2 Quantifying Storage in the Literature	10
2.3.3 Quantifying Uncertainty in the Literature	11
2.3.4 The Royal Society Report	12
Supply & Demand	12
Baseload	12
Supply & Demand Profiles	13
Efficiencies	13
Uncertainty	14
2.3.5 Consensus in the Literature	14
2.3.6 LDS in Practice	15
2.4 Identifying Meteorological Drivers	15
2.4.1 Meteorological Drivers in the Literature	16
Sudden Stratospheric Warming	19
Wind Stilling	20
2.4.2 Case Study: 1960s Blocking	20
3 Data & Methods	22
3.1 Scenario Modelling	22
3.1.1 Scenario Selection	22
3.1.2 Solar	24
3.1.3 Wind	24
3.1.4 Nuclear	25
3.1.5 Baseload	25
3.1.6 Supply	25
3.1.7 Demand	25
3.1.8 Supply-Net-Demand	26

3.2	Quantifying Storage	27
3.2.1	Storage Model	27
3.2.2	Quantifying Storage Capacity	28
3.2.3	Quantifying Uncertainty	29
	Monte Carlo Resampling	29
	Simulating Successive Depletion	29
	Varying Storage Efficiencies	29
3.3	Identifying Meteorological Drivers	30
3.3.1	Meteorological Data	30
3.3.2	K-Means Clustering	30
3.3.3	Cluster Analysis	31
4	Quantifying Storage	33
4.1	Supply-Net-Demand	33
4.2	Quantifying Storage Capacity	34
	Consensus with the Literature	36
4.3	Quantifying Uncertainty	39
4.3.1	Weather Uncertainty	39
	Monte Carlo Resampling	39
	Simulating Successive Depletion	40
4.3.2	Efficiency Uncertainty	41
4.3.3	Implications for Quantifying Storage Capacity	41
4.4	Further Comparison with the Literature	42
5	Identifying Meteorological Drivers	44
5.1	Case Study: Most Severe Depletion Event	44
5.1.1	Stage One: November 1958	44
5.1.2	Stage Two: December 1958	47
5.1.3	Stage Three: January 1959	48
5.1.4	Implications	48
5.2	Changing Drivers Across Scenarios	49
5.2.1	Changing Surface Conditions	49
5.2.2	Changing Depletion Drivers	50
5.3	Drivers Across the Historical Period	52
5.3.1	Consensus with the Literature	54
5.3.2	Clusters within a Historical Context	55
5.3.3	Consensus with the Literature	56
5.3.4	Clusters & Storage Capacity	56
6	Conclusions & Discussion	58
6.1	Conclusions	58
6.2	Discussion	60
	System Interactions	60
	Generalisability	60
	Temporal Resolution	61
	Net-Zero Scenario Modelling	62
	Supply and Demand Modelling	62
A	Literature Review	63
B	Data & Methods	65
B.1	Scenario Selection	65

B.2 Quantifying Storage Capacity	65
B.3 Demand	66
C Quantifying Storage	67
D Identifying Meteorological Drivers	68
Bibliography	69
References	69

List of Figures

2.1	2050 electricity supply pathways from three different Net-Zero reports.	9
2.2	Effect of simulation length on LDS capacity (Dowling et al., 2020)	11
2.3	Royal Society storage time series.	14
2.4	The four traditional North Atlantic-European weather regimes.	17
2.5	Increasing SST gradient between Ship Charlie and Ship India (Namias, 1964).	21
3.1	Wind power curves used by Bloomfield et al. (2022)	24
3.2	Supply, demand, and supply-net-demand profiles.	27
3.3	Storage Model Flow Chart.	28
3.4	Optimal k-means clustering parameters.	31
4.1	Supply, demand, and supply-net demand profiles for Headwinds.	33
4.2	Storage modelled from 1950-2022, with a detailed view from 1953-1964.	35
4.3	Distribution of the start and end (peak) dates of depletion events.	36
4.4	Storage capacity following the methodology of Dowling et al. (2020) . .	38
4.5	Distribution of capacity estimates derived from the Monte Carlo resampling method.	40
4.6	1950-2022 storage time series following The Royal Society's methodology.	42
5.1	Power variable anomalies and storage during the 1959 case study.	45
5.2	Mean meteorological field anomalies for the 1959 depletion event.	46
5.3	Mean spring-autumn 1958 anomalies for temperature, snowfall, and precipitation.	47
5.4	Composites of meteorological anomalies for all depletion events.	50
5.5	Supply, demand, and supply-net-demand power anomalies from 1959-1963.	51
5.6	Cluster centers from k-means clustering of depletion event composites.	53
5.7	The Headwinds scenario clusters over the 1950-2022 period.	55
5.8	Duration and required storage capacity of depletion events by cluster type.	57
5.9	Distribution of required storage capacity by cluster.	57
B.1	Electricity Supply for the Chosen Scenarios.	65
C.1	Required storage capacity for various system efficiencies.	67
D.1	Wind speed cluster centers from k-means clustering of depletion event composites for Headwinds.	68

List of Tables

3.1	Detailed overview of the three selected Net-Zero scenarios.	23
4.1	Annual mean and variance figures for supply, demand, and supply-net-demand for the three Net-Zero scenarios.	34
A.1	Brief overview of Net-Zero scenarios proposed by three key reports. .	63

Glossary of Terms

Abbreviations

BECCS	Bio Energy with Carbon Capture Storage
BEIS	Business Energy Industrial Strategy
CCC	Committee on Climate Change
CCS	Carbon Capture Storage
CREDS	Centre for Research into Energy Demand Solutions
DESNZ	Department for Energy Security and Net Zero
DJFM	December January February March
EU	European Union
FES	Future Energy Scenarios
GWL	Grosswetterlagen
LDS	Long Duration Storage
NAE	North Atlantic-European
NAO	North Atlantic Oscillation
PCA	Principal Component Analysis
RE	Renewable Energy
UK	United Kingdom

Terminology

Capacity Factor	Ratio of energy output over a period of time to the maximum possible output, used in reference to wind farms, solar farms, and other power generation facilities.
Required Storage Capacity	The energy capacity a long-duration storage system must have to meet all instantaneous energy deficits observed over a period of time, typically referring to the historical period.
Supply-Net-Demand	The surplus or deficit in energy supply after accounting for the total demand.
Watt-hour (Wh)	A measure of electrical energy equivalent to a power consumption or production of one watt for one hour.

Chapter 1

Introduction

In response to the escalating global climate crisis, forty countries in Europe, including the UK, have pledged to achieve Net-Zero carbon emissions by 2050 (Climate Watch, 2024). This ambitious target necessitates a profound transformation of national energy systems. Central to achieving this transformation is the decarbonisation of electricity generation, a significant greenhouse gas emitter, accounting for 14 % of 2020 greenhouse gas emission in the UK (Department for Energy Security and Net Zero, 2024, hereafter DESNZ). Decarbonising the electricity power sector is also relatively cost-effective compared to other sectors (Eggimann et al., 2020).

Since the 1980s, electricity generation from gas-powered turbines has played a key role in balancing electricity supply and demand across Europe (Hydrogen UK, 2023). However, as fossil fuels are phased out and variable renewable energy sources like wind and solar are phased in, the challenge of finding a large-scale replacement technology emerges. This shift, while driven by Net-Zero targets, is also motivated by substantial benefits. These benefits, discussed below, include enabling the electrification of heating, maximising the use of curtailed renewables, enhancing energy security amidst global volatilities, and facilitating the large-scale adoption of hydrogen.

Firstly, the National Grid anticipates that sectors such as heating and transport to undergo significant electrification by 2050. While the use of gas for heating is influenced by temperature but not limited by supply, electrifying heating will make electricity demand more temperature-dependent and variable (National Grid, 2023b).

Moreover, wind and solar energy, while relatively abundant, are subject to variability on timescales ranging from seconds to decades, with the North Atlantic Oscillation (NAO) being the leading mode of atmospheric variability in Europe (Marcheggiani et al., 2023). The intermittent nature of renewables means that electricity generation frequently exceeds or falls short of demand, resulting in curtailment costs and potential grid instability (Hydrogen UK, 2023). Pan-European atmospheric weather regimes can mean that periods of high demand and low supply can coincide for prolonged periods of time (Bloomfield et al., 2020b). Therefore, Long-Duration Storage (LDS) enables the storing of energy when production is high and demand is low, thereby enabling the use of otherwise curtailed renewable energy when supply is low.

The UK's dependence on natural gas and its relatively low gas storage capacity make it susceptible to global energy market volatilities, with recent UK energy crises

highlighting this vulnerability (Hydrogen UK, 2023). For example, the invasion of Ukraine caused significant disruptions in the European gas market, forcing many countries, including the UK, to reduce their dependence on Russian gas. According to Bolton (2024), this was followed by a sharp increase in gas prices, with typical energy bills for UK households still almost 30 % higher than pre-invasion levels. The unprecedented COVID-19 pandemic also impacted the availability of supply through supply chain disruptions, reduced workforce, and maintenance delays (Mulvaney et al., 2020). These events underscore the need for domestic measures to insulate the economy from such energy supply shocks.

Finally, there is a growing shift towards hydrogen due to its versatility and potential to be a cost-effective, low-carbon energy source. The Government's recent Energy Security Strategy acknowledged the vital role hydrogen will play in the UK's future energy mix by increasing the production target to 10 GW by 2030 DESNZ (2023). However, the development of LDS infrastructure is a prerequisite for achieving this production capacity, particularly in sectors such as heat and power generation.

This simultaneous increase in variability and volatility in both supply and demand poses significant challenges to maintaining a stable and reliable power supply. LDS technologies have emerged as a critical solution. LDS can store energy from renewable sources over extended periods—days, weeks, or even months—allowing energy to be used when renewable generation is low or demand is high (The Royal Society, 2023a). By replacing fossil fuels as a buffer, LDS could be key to ensuring a reliable, cost-effective energy supply while enabling a decarbonised future.

While much research has focused on short-term renewable energy intermittency and the need for LDS for buffering interannual variability, its application in smoothing decadal variability and the meteorological drivers of decadal variability in highly renewable energy systems remain less understood. As a result, there is a lack of consensus in the literature regarding the storage capacity required for nations transitioning to a Net-Zero energy landscape. This dissertation aims to bridge this gap by exploring the role of LDS in maintaining supply-demand balance in the whole-UK power system. This foresight will ensure that long-duration storage meets long-duration energy needs.

1.1 Motivation

This dissertation seeks to address key gaps in the current body of research in three main respects.

Firstly, various major organisations, including The Royal Society, the Committee on Climate Change (CCC), and the UK government's DESNZ, have published a range of projections and scenarios for the UK's future energy landscape. However, there is no consensus regarding the levels of supply and demand for 2050. Consequently, studies evaluating storage under a single Net-Zero scenario can yield widely varying estimates. This study aims to bridge this gap by reviewing the existing literature and adopting a comprehensive Net-Zero-centric approach to robustly quantify the range of plausible LDS capacities.

Secondly, ambiguity in capacity estimates has arisen because the meteorological drivers of storage depletion are poorly understood. This partly stems from the lack of consideration of a sufficiently long historical period. The Royal Society report (The Royal Society, 2023a), henceforth referred to as The Royal Society report, is one

of the most comprehensive studies focusing on LDS in the UK. This study examined 37 years of data from the 1980-2016 period. According to the Met Office, there is approximately a 10 % chance per decade of experiencing a winter month with wind speeds lower than those observed within that period (The Royal Society, 2023b). Using an additional three decades of reanalysis data, this dissertation suggests that there is approximately a 27 % chance of capturing at least one such extreme low wind speed winter month. Therefore, this study provides a more robust basis for quantifying LDS capacity.

Furthermore, much of the literature has a limited scope in explicitly accounting for uncertainties, such as the finite historical period and the unknown storage system conversion efficiencies to be implemented across the LDS fleet by 2050. This study attempts to quantify not only the required capacity but also to estimate a measure of uncertainty on top of that estimate.

Overall, this dissertation aims to provide a clearer understanding of the UK's storage needs and the meteorological drivers of such systems by addressing critical gaps in current research.

1.2 Objectives

Building upon the motivations outlined, this dissertation aims to answer the following research questions:

- 1. How much storage capacity will the UK require to meet energy deficits by 2050?**
 - (a) Does the required storage capacity vary depending on the pathway the UK takes to achieve Net-Zero?
 - (b) How do these estimates compare to those found in the existing literature?
- 2. What meteorological drivers govern the storage capacity required by the UK?**
 - (a) Do these meteorological drivers vary depending on the pathway the UK takes to achieve Net-Zero?

1.3 Outline

These outlined objectives are addressed in this study through Chapters 2 to 6.

Chapter 2 reviews the existing literature in three key areas: Net-Zero modelling, LDS estimates with a focus on the factors underlying the estimate from The Royal Society report, and meteorological factors affecting European energy systems.

Chapter 3 details the data sources and methodologies used to quantify storage capacity and identify meteorological drivers.

Chapter 4 presents a base estimate for storage capacity and additional estimates to address two types of uncertainty. It also includes a comparative analysis between the findings of this study and those of The Royal Society report.

Chapter 5 explores the meteorological drivers that influence the storage capacity estimates derived in Chapter 4, using a detailed case study spanning several years and a broader analysis over the historical period.

Chapter 6 discusses the broader implications of the findings from Chapters 4 and 5, and addresses sources of uncertainty and suggests directions for future research.

Chapter 2

Literature Review

This chapter reviews literature on Net-Zero energy system modelling, the principles behind LDS, and global LDS capacity estimates, with a focus on factors affecting The Royal Society's estimate. It then examines the meteorological drivers influencing energy systems and introduces a study relevant to a historical case study conducted later in this dissertation.

2.1 Flexibility

Achieving energy system flexibility is crucial to attaining a resilient, stable energy system, considering the inherent variability in both supply and demand.

Energy demand fluctuates due to several factors, including seasonal and daily variations driven by temperature and weather patterns, long-term trends in energy efficiency, and socio-economic factors such as the day of the week and commodity prices (National Grid, 2020). Additionally, global events like the 2020 pandemic (Mulvaney et al., 2020) and demographic changes such as population growth also impact energy demand (Roberts, 2008).

Energy supply can vary due to generation outages, scheduled maintenance, network constraints, and inaccuracies in demand forecasting (National Grid, 2020). The availability of energy sources also plays a role, necessitating the curtailment of wind turbines if wind speeds are too high or too low. Variable RE (renewable energy) generation is also location-specific and highly dependent on geographic and climatic conditions; for instance, solar power generation is affected by cloud cover and daylight hours (Hassan et al., 2023).

Enhancing flexibility within the energy grid is crucial for matching supply and demand despite their inherent variability. Different systems offer flexibility over various timescales based on their generation capacity, discharge duration, and ramp-up rates (Jenkins and Sepulveda, 2021).

As the UK advances towards its Net-Zero targets, renewable generation capacity must also increase, resulting in greater variability in generation output. National Grid (2020) notes that the increasing electrification of heat and transport will shift energy reliance from systems with substantial storage capacities, such as the gas network and petrol forecourts, to the electricity grid, which lacks comparable large-scale, on-site storage and relies on real-time generation.

The reduction in fossil fuels thereby eliminates a traditional source of supply-side flexibility. While hydrogen or gas generation with CCS can partially address this need, they alone are insufficient to manage the variability of renewable generation.

Therefore, the storage of energy from the electricity grid is essential for restoring grid flexibility.

Understanding energy system flexibility is a fundamental consideration in planning for the UK's transition to Net-Zero, and in turn, for LDS.

2.2 Net-Zero

Net-Zero entails balancing the emission of greenhouse gases with their removal from the atmosphere. It is intrinsically a scientific concept, based on the finite budget of carbon dioxide that can be allowed into the atmosphere. This budget, determined by climate science, is influenced by societal choices about acceptable temperature rises. Under the Paris Agreement, 197 countries have agreed to limit global warming to well below 2 °C and make efforts to limit it to 1.5 °C. Meeting these goals necessitates reaching net-zero CO₂ emissions by around 2050 (Fankhauser et al., 2022).

This balance can be achieved through emission reduction or emission removal via natural processes such as reforestation, or technological means like carbon capture and storage (CCS). However, while these technologies are clearly identified as solutions, the implementation pathway is complex, requiring operationalisation across varied social, political, and economic spheres. Numerous ethical judgements, social concerns, political interests, fairness dimensions, economic considerations, and technological transitions must be navigated (Fankhauser et al., 2022). Furthermore, the level of commitment to this target determines both the scale and pace of transformation required in the energy sector.

To explore and understand the pathways to achieve this goal, 'Net-Zero scenarios' are modelled, considering various projections for population growth, economic activity, and energy costs, often adopting a conservative approach to account for uncertainties. Consequently, these scenarios provide plausible frameworks rather than probabilistic solutions, with actual outcomes expected to fall between conservative and more optimistic projections.

In 2019, the UK became the first country to commit to a legally binding Net-Zero target, which has led to a relatively advanced body of scenario modelling research (Johnson et al., 2023). While these scenarios are devised based on various underlying assumptions, a typical 2050 Net-Zero scenario for the UK focuses on energy system flexibility, emphasising the shifting of demand and supply to align energy consumption with availability (National Grid; CCC, 2020; 2023):

- Demand-side flexibility:
 - Deployment of greenhouse gas removal technologies at scale, as well as carbon capture storage (CCS) at the point of emission, such as bioenergy with carbon capture and storage (BECCS) and fossil fuel combustion with carbon capture, such as gas with CCS.
 - Significant electrification of easy-to-treat sectors such as transport and heating, alongside continued decarbonisation of the power grid.
 - Increased switching to low-carbon fuels such as hydrogen and biomass in the most challenging areas to electrify such as heavy industry, aviation, and shipping.

- Implementation of available abatement options across natural resource sectors, including afforestation and low-carbon farming practices.
- Societal and consumer shifts towards embracing low-carbon alternatives and lifestyles changes to provide demand-side flexibility.
- Substantially improved energy efficiency of end-use technologies.
- Supply-side flexibility:
 - Electrification and increased adoption of hydrogen in the power sector. The former requires expansion and diversification of RE sources, enabled by the use of flexible and scalable generation methods such as pumped hydro and LDS. The latter necessitates significant hydrogen storage capacity to facilitate its adoption.
 - Improved energy efficiency in energy production technologies.
 - Development and deployment of smart grid technologies to dynamically balance and manage supply and demand.

From these measures, it is apparent that electrification and hydrogen adoption emerge as central supply and demand-flexibility strategies (National Grid, 2024).

Electrification involves using electricity as the primary energy carrier, often sourced from RE. It is particularly effective in sectors where direct electrification is feasible and the infrastructure is already suitable, such as in residential heating. In contrast, hydrogen adoption involves using hydrogen directly as an energy carrier to generate electricity or heat at the point of use, as opposed to being stored as in LDS. Hydrogen can be produced from natural gas reforming and RE through electrolysis, the same process used in LDS (Joffe et al., 2018). Hydrogen is especially valuable in sectors that are difficult to electrify directly (Hydrogen UK, 2023).

Electrification and hydrogen adoption are not mutually exclusive and can complement each other in the transition to Net-Zero, both necessitating the integration of LDS. Understanding the mutual impact of these flexibility measures proves crucial for broadening this study's findings to other potential Net-Zero futures.

2.2.1 Scenarios in the Literature

Given the inherent uncertainties in predicting the future, organisations model a range of Net-Zero pathways. However, each organisation may prioritise different parameters in their sub-scenarios, such as carbon emissions, technological advancements, societal attitudes, and policy shifts, resulting in distinct sets of scenarios that reflect varying focuses. To determine which scenarios are most grounded in realism and to assess the degree of consensus among them, a review is conducted of scenarios proposed by various organisations.

For instance, the CCC, a statutory body that advises the government, published a report which explores four pathways characterized by varying levels of technological and social change. These four pathways inform a central Balanced Pathway, which is constructed to keep in play a range of ways of attaining Net-Zero. For example, this pathway balances the use of both electrification and hydrogen adoption for home heating (CCC; CCC, 2020b; 2020c).

The Centre for Research into Energy Demand Solutions (CREDS) released the Positive Low Energy Demand report in 2021, outlining four demand scenarios. One scenario reflects adherence to current policies through 2050, providing a baseline for comparison against more ambitious pathways (Barrett, 2021).

The National Grid (NG) published National Grid (2023b), which outlines four Net-Zero pathways, defined by the speed of societal and decarbonisation changes. The pathways range from a minimally ambitious approach, focused solely on supply-side flexibility, to a highly ambitious approach that integrates both supply-side and demand-side flexibility alongside significant societal shifts.

The 'Build Back Greener' report by DESNZ (2021) outlines three pathways that adopt a flexible approach to supply. These scenarios include extensive electrification of transport and heating, and the decarbonisation of electricity supply through nuclear power and greenhouse gas removal technologies. One scenario explores the role of hydrogen in power and transport, combined with land-use sinks. Another anticipates substantial innovation, enabling low emissions and extensive deployment of greenhouse gas removal technologies.

Consensus in the Literature

From the literature, the NG, CCC, and CREDS reports were identified as having the clearest documentation, both in terms of narrative descriptions and the quantitative data on supply and demand levels across different sectors. These reports are therefore suitable for establishing the expected boundaries of demand and supply for 2050. The sources and corresponding electricity generation are illustrated in Fig. 2.1. All referenced figures are derived from CCC; National Grid; CREDS (2020a; 2023a; 2022).

The figure reveals that the CREDS scenario features a disproportionately high share of onshore wind generation within its renewable energy mix. While both the CCC and NG scenarios suggest onshore wind shares below 22 %, the CREDS scenario reports proportions ranging from 34 % to 42 %, a level comparable to its offshore wind generation. Additionally, the CREDS scenario exhibits overly ambitious reductions in both generation and final demand, as noted by Johnson et al. (2023).

In contrast, the NG and CCC scenarios exhibit a level of consistency that allows for the construction of analogous scenarios for comparative analysis. For example, NG-FS and CCC-H can be considered analogous lower-ambition scenarios. Both are characterised by limited societal change, a focus on the electrification of transport rather than heating, and a reliance on supply-side flexibility and carbon dioxide removal technologies to achieve Net-Zero. They suggest a range of 660 TWh to 690 TWh for electricity supply and 550 TWh to 570 TWh for demand.

Similarly, NG-ST and CCC-BP represent moderately ambitious scenarios with comparable levels of societal change. They emphasise supply-side flexibility with low to moderate efficiency improvements. NG-ST leans towards hydrogen for heating, while CCC-BP maintains a more balanced approach between hydrogen and electrification of heating. Their scenarios suggest an electricity supply range of 780 TWh to 785 TWh and a demand range of 620 TWh to 680 TWh.

Lastly, NG-CT and CCC-WI reflect the more ambitious end of the Net-Zero spectrum. Both scenarios feature high levels of electrification in heating, though they

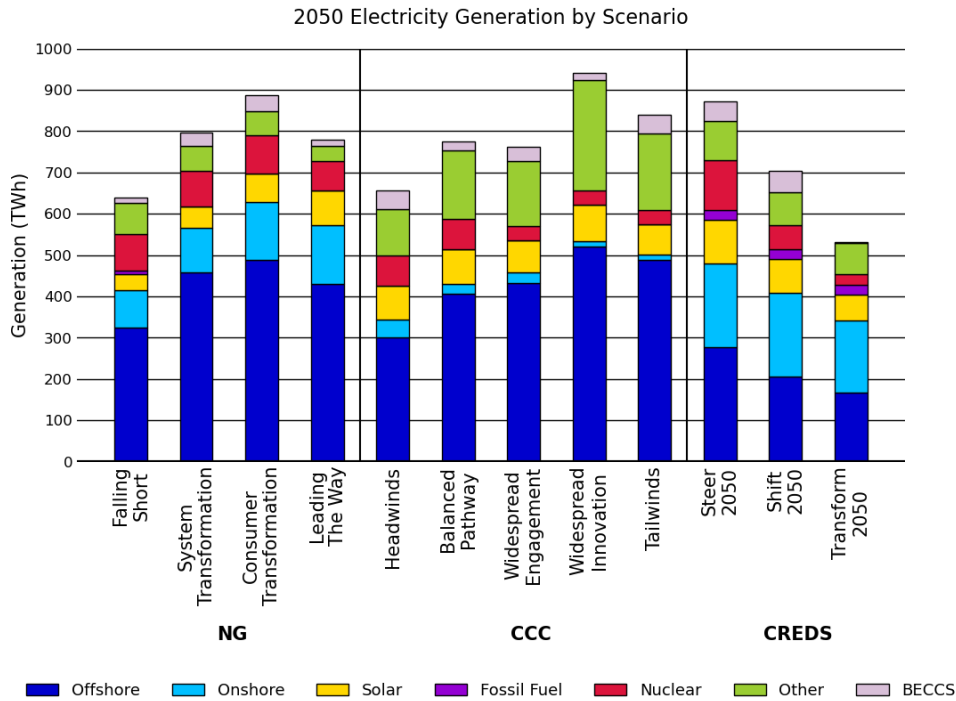


FIGURE 2.1: Electricity generation in 2050 for Net-Zero scenario collections reported by the National Grid, Committee on Climate Change, and Centre into Research for Energy Demand Solutions. Data adapted from CCC; National Grid; CREDS (2020a; 2023a; 2022).

differ significantly in terms of societal change. They suggest an electricity supply range of 910 TWh to 940 TWh and a demand range of 680 TWh to 730 TWh.

To summarise, the estimated boundaries for electricity supply are 680/780/930 TWh, and 560/650/700 TWh for demand. These estimates provide a valuable framework for understanding the modelling assumptions of The Royal Society report, which informs the methodologies in this study.

2.3 Quantifying Storage

Before examining the storage estimates detailed in the literature, the fundamental principles of LDS are outlined.

2.3.1 LDS Principles

LDS technologies provide a means of storing energy over extended periods, ranging from days to weeks and potentially up to decades, and can sustain electricity provision for prolonged durations from days to weeks (Science and Technology Committee, House of Lords, 2023). These technologies encompass both conventional and novel approaches, including mechanical, thermal, geochemical, and electrochemical storage, each at varying levels of maturity with significant efficiency advancements projected by 2050 (H2eart for Europe, 2024).

LDS offers a compelling alternative to short-term storage options like lithium-ion batteries and pumped-storage hydropower. Unlike these technologies, which often

have fixed relationships between charge and discharge capacities, LDS can separate these two components. This separation allows LDS to independently manage and optimise both the quantity of energy stored and the rate at which it is discharged (Jenkins and Sepulveda, 2021). Among the most promising forms are underground gas storage options, such as hydrogen storage in salt caverns. These caverns serve as resilient, protected, and relatively leak-proof reservoirs for hydrogen storage (Storage Working Group, 2022). Due to the higher volatility and production costs associated with ammonia, hydrogen emerges as the leading candidate for energy systems (The Royal Society, 2023a), making it the primary focus of this dissertation.

Renewable electricity is converted to hydrogen via electrolysis, with some losses, and stored underground at pressures of approximately 300 hPa to 800 hPa, incurring minor leakages. A fuel cell or a four-stroke engine converts the hydrogen back into electricity, with a round-trip efficiency of approximately 41 % (The Royal Society, 2023a).

2.3.2 Quantifying Storage in the Literature

Estimating the required LDS capacity for the UK's energy system has produced a wide range of results, mainly due to the different use-case assumptions employed in each study.

Scafidi et al. (2021) used 2019 UK gas demand data from Ofgem and suggested that if the UK were to fully convert its gas network to hydrogen, at least 150 TWh of hydrogen storage would be required to meet inter-annual variability in demand. However, the study acknowledges it did not account for potential contributions from nuclear energy and interconnections.

Mouli-Castillo et al. (2021) estimated that if only the decarbonisation of the domestic heating sector is considered, the storage requirement would reduce to 78 TWh. This estimate assumes that the existing gas distribution network can be repurposed for hydrogen transport, implying that significant investments in new infrastructure may not be necessary, thus making LDS a more feasible option. The study focuses solely on inter-annual variability in heating demand.

In its most recent July 2024 report, the National Grid's Future Energy Scenarios report proposes four revised pathways to those discussed in Section 2.2.1. Their Hydrogen Evolution pathway obtains most of its flexibility from hydrogen storage, with 49 TWh projected for 2050, with all other scenarios requiring less than 20 TWh (National Grid, 2024).

On the lower end of the spectrum, a report by the Department for Business, Energy Industrial Strategy (2023, hereafter BEIS), commissioned to AFRY Management Consulting—which also provided the demand model for The Royal Society report—estimated a 2050 requirement of approximately 11 TWh to 17 TWh. The report notes that oversizing this capacity by 5 TWh would be a 'low regret' decision, adding extra resilience to the energy system.

Similarly, the CCC (2023) report, also commissioned to AFRY, found that 7 TWh to 12 TWh of LDS is required by 2050. The report argues that the role of hydrogen for seasonal storage may not be significant by 2050, as electricity supply is expected to primarily come from offshore wind during winter. Instead, LDS is proposed as a long-term backup solution for extended periods of low-wind generation or power outages. The report highlights that hydrogen demand in the power sector is a strong

determinant of the scale of hydrogen storage required, with intermittent sources of hydrogen demand requiring more storage compared to more stable sources like industry.

Kimpton et al. (2023) found that a hydrogen store of 29 TWh to 65 TWh would be required to ensure continued energy provision during the coldest periods with very low wind generation. Similar to the CCC's findings, scenarios with more hydrogen heating require more LDS, but those with electrified heating require more electricity generation and transmission infrastructure.

Dowling et al. (2020) simulated the United States' need for LDS and found that increasing the simulation period significantly impacts storage needs. Their findings were reported in terms of demand hours—how long storage can supply the average demand—rather than traditional energy capacity metrics. However, they found that in a 6-year simulation, the median energy capacity for LDS was 85 % greater compared to a 1-year simulation.

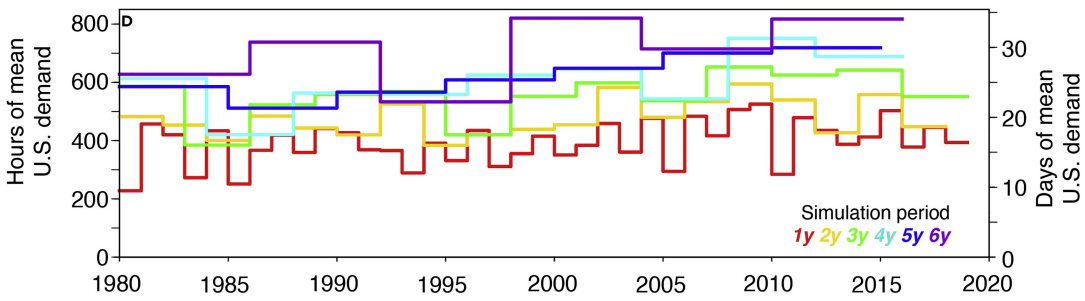


FIGURE 2.2: Effect of simulation length on LDS capacity over the 1980-2020 period from Dowling et al. (2020), expressed in hours of mean United States' demand. The horizontal lines represent the optimised LDS capacity for that time period, based on minimising system costs, while ensuring 100 % reliability.

The variation in storage estimates across the literature and their underlying assumptions makes it challenging to quantify the actual need for LDS. However, several key points emerge:

- **Scale:** Most studies agree that achieving Net-Zero in the UK by 2050 will require tens of TWh of storage, with estimates generally lower than that by the RS. While exact figures differ, the need for substantial storage capacity is widely acknowledged. Generally, studies which do not explicitly model nuclear, BECCS, geothermal or battery storage tend to return higher estimates (> 50 TWh).
- **Temporal Scope:** The majority of studies emphasise the importance of storage on an inter-annual basis, with few addressing needs over decadal timescales. In the cited literature, weather data is generally used only from the 1970s onwards.

2.3.3 Quantifying Uncertainty in the Literature

A review of the existing literature reveals that no other studies explicitly quantify the uncertainty in LDS capacity in a similar manner. However, broadening the review to power system modelling reveals common uncertainty quantification methods that

can be adapted for underground hydrogen storage. By considering the underground hydrogen storage model in this dissertation as a type of power system model, then according to Hilbers et al. (2020), its input variables, such as supply-net-demand, can be considered as samples from an underlying distribution, and are thus subject to sampling uncertainty. Therefore, a Monte Carlo sampling method could be used to estimate the probability distribution of the output of a storage model. This approach involves randomly sampling supply-net-demand values based on their assumed probability distributions, and using these samples as inputs to a storage model.

2.3.4 The Royal Society Report

This study places particular emphasis on The Royal Society report due to its recent publication and comprehensive documentation. The report incorporates key assumptions at various stages, from the initial scenario construction to the modelling of storage requirements, each of which contributes to the final storage estimate.

Supply & Demand

At its most foundational level are its assumptions regarding electricity supply and demand in 2050. The report assumes mean annual demand to be 570 TWh which aligns with the lower boundary identified in Chapter 3. The report acknowledges that such a level is indicative of significant improvements in efficiency and societal change, but with a lesser degree of electrification of space heating. Thus, this implies that it is analogous to a combination of the Headwinds and Balanced Pathway scenarios.

In terms of supply, the report assumes an ambitious 100 % of supply will be sourced from RE with no baseload power, which contrasts with the selected CCC scenarios, which comprise of RE shares of 75 % to 90 %. This, however, suggests that The Royal Society assumes a highly advanced energy grid akin to Widespread Innovation.

Furthermore, The Royal Society report concludes that the assumed demand can only be met with hydrogen storage if the RE supply exceed 704 TWh yr^{-1} , as so the report assumes a mean annual supply of 741 TWh yr^{-1} . This supply figure level lies between that of Headwinds and Balanced Pathway. However, those scenarios include some baseload power, and therefore their RE supply ranges from

Thus, the report assumes this as the 2050 level of supply, a figure, which, again, aligns with a supply level between that of Headwinds and Balanced Pathway. However, those two scenarios contain a baseload, and so their supply from RE actually ranges from 427 TWh yr^{-1} to 623 TWh yr^{-1} . The high RE shares and overall high RE supply level in The Royal Society report imply very high installed capacities would be required to realise such a scenario.

Baseload

Within its supplementary document, The Royal Society conducts an additional analysis containing a static baseload. They found that such an inclusion reduces the required storage capacity estimates by 27 %. They explain that the inclusion of a nuclear baseload in particular, mean that when there is a deficit, nuclear generation can cover this deficit, with the remaining able to make hydrogen, and when there is a surplus, all nuclear can also be used to make hydrogen when the store is not full.

Therefore, by not including any form of baseload within their main study, they have not accounted for reductions in storage.

Given that the NG and CCC scenarios all call for some level of baseload, such an inclusion is crucial. Furthermore, the baseload which they did model was a static baseload. Nuclear is a flexible generation source, meaning that it can ramp up or down to balance supply and demand, thereby having their own annual cycle that mimics seasonal demand patterns. Excluding this variability could lead to a particular underestimation of supply during periods of high demand, particularly in winter, and consequently, an overestimation of the required storage capacity. In a scenario like Headwinds, this effect may be most pronounced in Headwinds as it has a high share of baseload within its supply mix. Conversely, in a more advanced scenario like Widespread Innovation scenario, although nuclear supply is generally lower, its inclusion could potentially counter the increased winter surge in demand, again, mitigating an underestimated storage capacity.

Supply & Demand Profiles

Aside from the mean-annual supply and demand figures, the report makes assumptions regarding their actual profiles. The Royal Society report uses a repeated time series of the 2018 year of demand, inclusive of weather effects. This time series was scaled up to a mean annual demand levels (570 TWh), assuming no interannual variability in demand and no further electrification variability from 2018-2050. The study found that correlations between supply and demand were sufficiently low such that when interannual variability in demand was accounted for post-publication, the increase in storage capacity was 10 %. This was deemed acceptable as it was within the suggested 20 % contingency.

The implications of applying these assumptions to the Net-Zero scenario of this study are explored in Section 4.4.

Efficiencies

Additionally, The Royal Society report's assumptions of high-end projections of input, output, and storage efficiencies.

The report assumes a value of 74 % during the electrolysis. The report studies considers 4 different types of electrolyzers, citing a 2017 study which reveals that most of a group of experts favouring Polymer Electrolyte Membrane electrolyzers. It notes that efficiencies of 74 % and from 67 % to 74 % are expected by IRENA and IEA, respectively by 2050. However, if LDS is to be installed at a large-scale by 2050, the fleet will be built over a prolonged period of time, and so the 2050 installed LDS will likely not have such a top-end 2050 efficiency.

For the conversion of hydrogen to electricity with a four-stroke engine. The report considers fuel cells widely used today. They have efficiencies from 45 % to 62 %, with The Royal Society report opting for the Hydrogen Proton Exchange Membrane fuel cell efficiency of 55 %. However, the report notes that none of these are currently deployed for grid scale projects. Det Norske Veritas (2022) notes that additional development with PEM goes to the reduction and recycling of iridium and platinum, rare materials which could limit very large-scale expansion of PEM. The Kansas project, mentioned earlier, reports an efficiency of approximately 44 %."

The report justifies its assumption of 0 % hydrogen leakage during electrolysis and storage, citing a DESNZ and BEIS (2022) report that it would be relatively easy and feasible to incorporate technology to catch and recombine the lost hydrogen. With a 50 % to 99 % confidence interval that analysis suggests an electrolyser-storage-fuel cell leakage of 1 % to 3.5 %. There is a lack of alternative leakage studies in literature currently.

The report acknowledges that these input and output efficiencies are highly dependent on various factors, including output power, storage levels, temperatures, pressures, and the number of battery cycles. Given these uncertainties, a more conservative approach to selecting efficiencies would have been prudent.

Uncertainty

To account for the various sources of uncertainty discussed, particularly those arising from weather and climate vagaries not captured within its 37-year supply dataset, The Royal Society report suggests an additional 20 % contingency in their 100 TWh storage capacity estimate. However, the report does not provide a justification for the specific 20 % figure. The base estimate - the magnitude of storage between full capacity and maximum depletion - and the contingency are visualised in the report's modelled capacity time series, shown in Fig. 2.3.

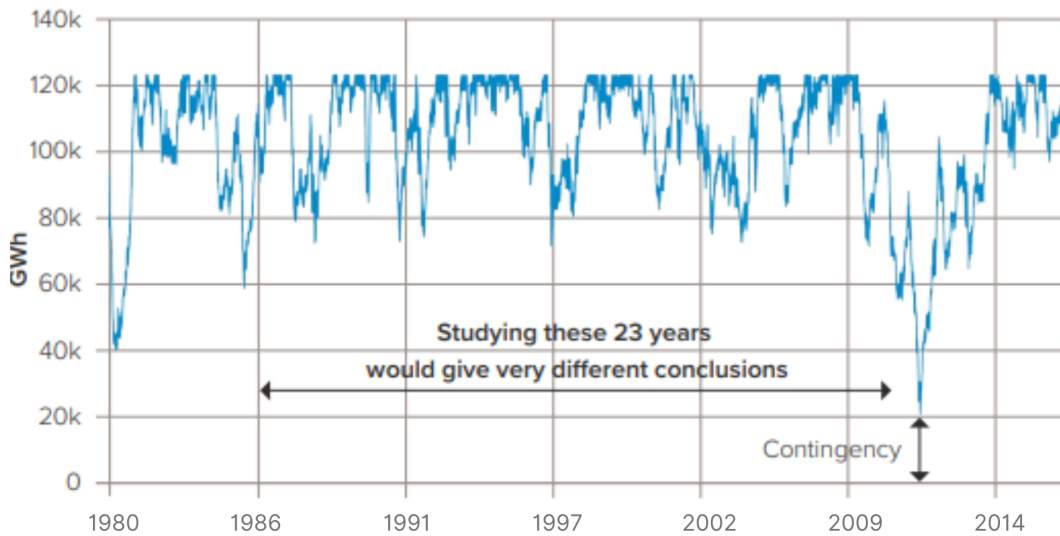


FIGURE 2.3: The 1980-2018 storage capacity modelled in The Royal Society's The Royal Society (2023a).

2.3.5 Consensus in the Literature

While Net-Zero frameworks are inherently speculative, the RS's scenario lacks internal consistency. Its assumptions regarding demand, supply, installed capacities, energy shares, and efficiencies represent differing levels of progression in the UK's energy grid. This dissertation demonstrates how such misplaced assumptions can lead to inflated estimates of storage, which are addressed in the following ways:

- By focusing solely on the most plausible Net-Zero scenarios, This study refines the range of scenarios presented in the literature review to select those with reasonable underlying assumptions.

This approach aligns with the National Grid's recent emphasis on realism, as highlighted in their National Grid (2024) report.

- By modelling a non-100 % RE scenario, by including of a baseload, with a dynamic nuclear component.
- By accounting for interannual variability and the electrification of demand.
- By considering a longer historical period to capture a more comprehensive range of weather conditions.

2.3.6 LDS in Practice

The UK has the first globally deployed hydrogen storage salt caverns located in Teesside since 1972. Although it is still currently the only commercially operational underground hydrogen storage cavern in the UK, other sites offer a potential storage capacity of up to 9 PWh (Hydrogen UK, 2023).

In addition to salt caverns, Mouli-Castillo et al. (2021) also estimated that total geological storage capacity in selected offshore gas fields, for use in LDS, is approximately 2662 TWh, significantly higher than their estimated 78 TWh for the decarbonisation of gas.

The European Network of Transmission System Operators for Gas has published a Hydrogen Infrastructure Map, detailing 50 hydrogen storage pilot projects set to be commissioned between now and 2040. These projects combine to an intended capacity of 9.1 TWh by 2030 and 22.1 TWh by 2040. Approximately two-thirds of these will be in salt caverns, with the remainder in depleted gas fields, aquifers, and rock caverns (H2eart for Europe, 2024).

Various EU and national funding initiatives are supporting the development of large-scale hydrogen storage. Notably, the FrHyGe project, launched in 2024 with €43 million from the European Union, aims to validate industrial-scale hydrogen storage (Storengy, 2024). Additionally, the European Commission allocated nearly €720 million in subsidies to seven green hydrogen projects in 2023, with more funding anticipated (Pearce, 2024).

Underground hydrogen storage is currently the only 'proven' technology for LDS at scale, making it the most mature option for meeting the UK's energy needs (Arup, 2023). Despite this, as well as significant funding and growing interest, the planned storage capacity still falls short of the broad range of estimates from the literature, not just in the UK but across Europe. Furthermore, the planned storage capacity for Europe often surpasses the storage estimates suggested for the UK alone, indicating a lack of consensus regarding the storage needs for both regions. Given the substantial time and capital required to deploy large-scale storage projects, along with the urgent near-term demand, the need for LDS represents an immediate challenge rather than a future concern (Arup, 2023).

2.4 Identifying Meteorological Drivers

Recognising the meteorological drivers of energy systems and their evolution with changing energy landscapes is crucial not only for effectively balancing current

supply and demand but also for determining the most resilient and safest energy systems to transition to in achieving Net-Zero goals.

Transitioning to a weather-dependent electricity system can impact both supply and demand, thereby introducing challenges related to both oversupply and under-supply of renewable generation. During periods of high renewable generation and low demand, oversupply can lead to lower system prices, incentivising increased demand or charging of LDS units to reduce the risk of curtailing generation. On the other hand, extended periods of low weather-dependent generation, such as during 'dunkelflaute' events, combined with high demand for cooling in summer or heating in winter, can strain energy systems. These extended periods could exhaust shorter-term battery storage options, necessitating flexible generation technologies such as LDS to ensure security of supply.

This is particularly crucial when considering seasonal or even decadal variability, which can exacerbate these effects over longer timescales. Moreover, wind droughts and extreme low temperatures can occur on a pan-European scale, leading to simultaneous power deficits across Europe and the UK. This synchronicity diminishes the effectiveness of interconnectors in balancing demand, as neighbouring regions may not have surplus to spare (Wohland et al., 2017). Therefore, understanding these meteorological patterns is also essential for effective interconnection planning.

The types of energy infrastructure installed also affect the system's vulnerability to different meteorological drivers. High installations of solar power, for example, create a pronounced annual cycle of energy supply, increasing vulnerability to low-solar periods. Conversely, a high reliance on wind power introduces significant variability across many timescales, heightening vulnerability to low-wind periods (Bloomfield et al., 2018).

Overall, understanding the magnitude, frequency, duration, and synchronisation of meteorological impacts across Europe allows for better anticipation of fluctuations in supply and demand, thereby enhancing the resilience of energy systems.

2.4.1 Meteorological Drivers in the Literature

The exact meteorological drivers of energy system imbalances are often complex. As Net-Zero requires a transition to a weather-dependent energy system, two challenges arise. Firstly, the influence of meteorological conditions on the energy system is expected to intensify with the increased deployment of RE sources (van der Wiel et al., 2019). Secondly, predicting these dynamics becomes increasingly difficult due to the inherent uncertainties in predicting the future energy landscape (The Royal Society, 2023b). This section explores how these meteorological drivers are currently identified in the literature.

Circulation weather types, or regimes, classify meteorological events by defining synoptic-scale patterns based on climate variables like temperature, precipitation, and wind speed. These quasi-stationary and recurrent patterns modulate surface weather over multi-day to weekly timescales (Michelangeli et al., 1995), significantly affecting the European energy sector (Bloomfield et al., 2020b).

From such approaches, four fundamental winter weather regimes are commonly identified for the Euro-Atlantic region: the positive and negative phases of the

NAO, the Atlantic Ridge, and Scandinavian Blocking. Van Der Most et al. (2022) identified these regimes and investigated their impacts on wintertime mean and extreme wind and solar power production, temperature-driven energy demand, and energy shortfall. These regimes are illustrated in Fig. 2.4. The findings for each regime are:

- **NAO negative (NAO-):** Corresponds to a blocking system situated over Greenland and Iceland, leading to reduced zonal flow over the northern half of Europe, in particular, a reduction in 10m wind speeds in the northern North Sea and North Atlantic, as well as colder temperatures.
- **NAO positive (NAO+):** Features a low-pressure system over Iceland and higher pressure to the south, resulting in stronger west-to-east winds. This regime typically leads to higher than normal 10m wind speeds over the North Sea, Denmark, Ireland, the Netherlands, and the United Kingdom.
- **Atlantic Ridge:** Characterised by high pressure over the North Atlantic and low pressure over Europe, affecting weather patterns and wind flow. The impacts on 10m wind speeds are generally less pronounced, with slight increases over the Mediterranean Sea and North Sea.
- **Scandinavian Blocking:** Involves high pressure over Scandinavia and lower than normal pressure to the south and west, reducing zonal wind flow and impacting wind speeds across the North Sea, the Celtic Sea, and the Bay of Biscay. This regime results in lower than normal 10m wind speeds over these areas and higher incoming solar radiation over France.

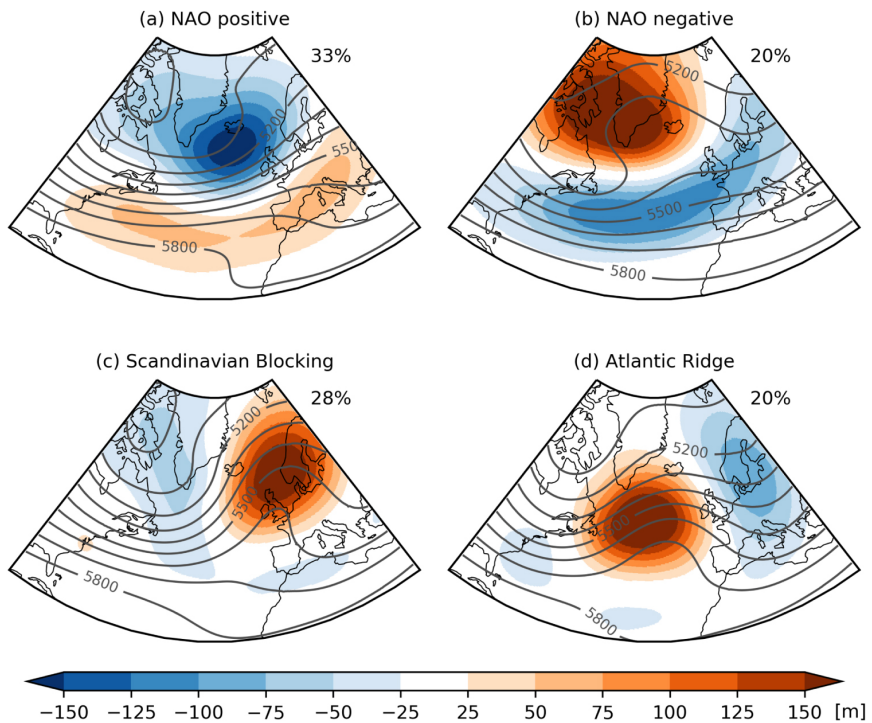


FIGURE 2.4: The four traditional North Atlantic-European weather regimes, indicated by the DJF 500 hPa geopotential height anomaly (Van Der Most et al., 2022). The percentages indicate the proportion of the total days studied within each regime.

Van Der Most et al. (2022) also found that days with a blocked circulation pattern, specifically the Scandinavian Blocking and NAO- regimes, generally have lower than normal renewable power production and higher than normal energy demand, leading to increased energy shortfall. It also defined extreme high energy shortfall events, those with a combination of both low wind and low solar power production, and high energy demand, and found that their occurrence increases by a factor of 1.5 and 2.0 during Scandinavian Blocking and NAO- regimes, respectively. Van Der Most et al. (2022) notes that while extreme high shortfall events are more likely during blocked regimes, they are driven by rare circulation types and small-scale features rather than common large-scale circulation types.

Another study by Mockert et al. (2023), considered the impact of low wind speeds and insolation, termed Dunkelflauten, meaning 'dark wind lulls', and quantified their impact on German energy systems. A study of these periods in Germany revealed most Dunkelflauten can be attributed to a high-pressure system over Germany, noting that the NAO- blocking is associated with colder temperature and therefore higher electricity demand, and may present a challenge with the expected electrification of space heating.

The study emphasises the importance of considering the broader meteorological context to understand such periods. For example, during Scandinavian Blocking and Greenland Blocking Dunkelflauten, Germany is situated in the center of a quadripole patters. In the latter, a low-pressure systems are located over the Atlantic north of the Azores and Scandinavia, and high-pressure systems extend over the Icelandic region and southeastern Europe. This quadripole is responsible for advecting cold air towards Europe before the onset of the Dunkelflauten, resulting in significant negative temperature anomalies across Germany and Northern Europe.

Finally, the study notes that Dunkelflauten occur predominantly when a weather regime is well established and persists longer than usual, emphasising the importance of both the type and duration of meteorological conditions.

Brayshaw et al. (2012) alternatively uses Grosswetterlagen (GWL) regimes to discuss the meteorological patterns associated with high demand and low wind conditions. The Grosswetterlagen classification is set of 29 European weather regimes, used widely in synoptic meteorology for both forecasting and climatology. According to Lee et al. (2020), GWL regimes capture finer, localised differences more effectively than the four classical regimes, but notes that they are not mutually exclusive and can co-occur. The study by Brayshaw et al. (2012) identifies three distinct circulation types that drive winter peak demand in Great Britain:

- **High-over-Britain Anticyclone (HB):** This regime is generally associated with very low wind speeds but relatively moderate temperatures. This study suggests that while HB can contribute to peak demand in any given year, it is not the regime most likely to cause the highest demands when looking over multi-annual timescales.
- **Blocking Over Scotland/Scandinavia (HNFZ/HNFA/HNA/HNZ):** These regimes conditions often bring cold air from the continent into Great Britain, leading to higher demand for heating.
- **Latitudinally Extended Troughs Over Western Europe (TRW/TRM/TM):** The trough patterns can cause cold air advection from northern/central Europe

towards Great Britain. They are associated with high demand events, although the wind resource in these conditions can vary.

Grams et al. (2017) finds that blocked regimes (Atlantic Ridge, European Blocking, Scandinavian Blocking, and Greenland Blocking), stationary anticyclones disrupt the mean westerly flow into Europe, therefore reducing wind power output over regions like the UK and enabling cold conditions to prevail. It finds that, while European Blocking results in weak winds across vast parts of Europe, such stationary anticyclones can be flanked by anticyclonic activity, resulting in enhanced winds in peripheral regions like northern Scandinavia and the Balkans.

A review of the literature indicates that blocking systems, especially prolonged ones, in the vicinity of the UK (such as High over Britain, Scandinavian Blocking, and NAO- regimes) have the potential to significantly impact both wind supply and electricity demand across the UK simultaneously.

Sudden Stratospheric Warming

Sudden Stratospheric Warming (SSW) events can significantly influence weather regimes and surface conditions in the North Atlantic-European (NAE) region for several weeks. SSWs are caused by the breaking of planetary-scale waves that propagate upwards from the troposphere, leading to the weakening or reversal of the polar vortex. This weakening reduces the strong westerly winds that typically maintain a zonal flow pattern in the jet stream. As a result, the jet stream experiences more pronounced meridional movements, which can lead to the formation of large-scale ridges and troughs. These features can become stationary or quasi-stationary, resulting in blocking patterns, such as a Blocking High over Greenland.

While SSWs occur approximately every second winter, their tropospheric and surface responses can vary greatly. For instance, the SSW in early 2018 triggered the 'Beast from the East', bringing severe cold and heavy snowfall to much of Europe. Conversely, the SSW in 2019 led to relatively mild temperatures across Scandinavia (King et al., 2019).

Despite this variability, typical responses to SSWs include a prolonged negative NAO phase and a switch from a positive to a negative NAO phase (Domeisen, 2019). Charlton-Perez et al. (2018) observed more frequent transitions towards NAO- following SSW events. Additionally, Karpechko et al. (2018) noted that a mid-February 2018 SSW event may have 'preconditioned' the atmosphere, leading to the NAO transition that triggered the February-March 'Beast from the East'.

Conversely, blocking systems can precondition the atmosphere for the occurrence of an SSW by enhancing the upward propagation of planetary waves that disturb the polar vortex. The study by Martius et al. (2009) indicates that nearly all major SSW events are preceded by blocking patterns in the troposphere. Specifically, blocking events over the Atlantic basin, including Scandinavia, are often precursors to vortex displacement SSW events.

In terms of surface effects, Winters with SSWs tend to be colder than average in areas like Scandinavia. King et al. (2019) found that below-average temperatures often precede SSW events, but the cold extremes are more intense in the 60 days after the SSW.

This study will later suggest a scenario where a blocking event preconditions the atmosphere for an SSW, which then sets the stage for an NAO- transition, leading to cold, low-wind speed weather conditions.

Wind Stilling

Previous sections have discussed prolonged periods of low wind lasting days to weeks, and their impact on energy systems. This section addresses the phenomenon of multi-annual to decadal periods of wind drought, often known as wind stilling, which is a gradual decrease in surface-level wind speed over these extended time scales (Masson-Delmotte et al., 2021).

The Sixth Assessment Report by the Intergovernmental Panel on Climate Change (IPCC) indicates 'low to medium' confidence in the detection of historical wind stilling and its attribution to specific causes. This uncertainty arises primarily from the short duration and inhomogeneity of the observed wind stilling series (Masson-Delmotte et al., 2021).

Zhou et al. (2022) sought to address uncertainties in historical wind speed data by constructing a century-long homogenised wind speed series using observations from 13 stations in Sweden. Their findings indicate two periods of prolonged wind stilling. The first occurred during the 1950s and 1960s, and the second, of much greater magnitude, from 1990 to 2005. During the latter period, wind speeds dropped significantly, falling below the levels observed during the 1960s stilling from 1995 to 2005. Subsequently, wind speeds showed a very quick recovery post-2005, indicating a strong reversal of the previous stilling trend.

The causes of wind stilling have been widely debated in the literature, with factors such as urbanisation and land-use changes (Vautard et al., 2010), large-scale atmospheric circulation changes (Zeng et al., 2019), and blocking regimes like the NAO being proposed (Minola et al., 2016). The Royal Society's supplementary information highlights the link between wind stilling and the NAO, noting that wind speeds were generally lower from 1960–1980 than from 1980–2016 due to atmospheric blocking associated with the NAO-. During these periods, positive phases of the NAO were less frequent and had a smaller amplitude (The Royal Society, 2023b).

Given the high levels of wind deployment in the Net-Zero modelled scenarios discussed in Section 2.2.1, wind stilling is a phenomenon that should be considered when planning for LDS deployment. This study's subsequent analysis of the meteorological drivers of LDS depletion reveals a discernible influence of wind stilling on LDS.

2.4.2 Case Study: 1960s Blocking

A study by Namias (1964) examines a persistent blocking period over Northern Europe from late 1958 through 1960. This dissertation later discusses the practical implications of these drivers on a Net-Zero energy system.

The study suggests that an unusually strong north-to-south transport from the North Atlantic to Northern Europe during winter set in motion a complex chain of events leading to successive seasons of atmospheric blocking. This blocking was maintained by a positive feedback loop involving North Atlantic sea surface temperatures and snow in the Scandinavian Peninsula.

During this blocking period, the vicinity of Ship Charlie (location indicated in Fig. 5.2 became significantly colder-than-normal, while the area around Ship India became warmer-than-normal, with a mean difference of 4°C between the two. The temperature anomalies computed by Namias (1964) are shown in Fig. 2.5.

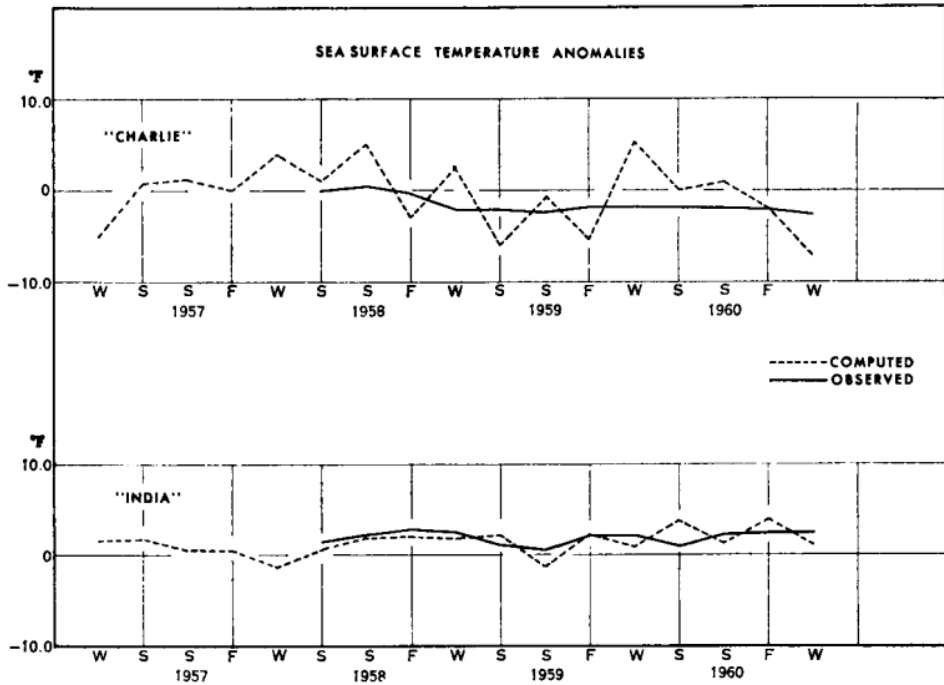


FIGURE 2.5: Sea surface temperature anomalies observed and computed at Ship Charlie and Ship India by Namias (1964). Note the increasing temperature gradient between the two from spring 1958 to 1959.

Namias (1964) suggests that temperature anomaly strengthened the southerly component of the thermal wind in the lower troposphere, enhancing the east-to-west temperature gradient. This led to increased frontogenesis and greater development of storms making up the westward-displaced Icelandic Low (a semi-permanent centre of low atmospheric pressure found between Iceland and southern Greenland). In response, storm paths that would typically move eastward were displaced northward, favouring the development of high-pressure ridges over Northern Europe.

The study proposed an a priori hypothesis that warm-season blocking could be encouraged by a warmer-than-normal Scandinavian Peninsula, which would enhance thermal contrasts with the Atlantic Ocean and the Baltic Sea. It also suggested that reduced snowfall would lower the region's albedo, increasing solar radiation absorption and potentially encouraging ridge formation, similar to the Indian monsoon. Additionally, reduced precipitation could result in lower snowpack, indicating a complex feedback mechanism involving sea surface temperature gradients, precipitation, snow cover, and ridge formation. This study will later examine the hypothesis proposed by Namias (1964) using reanalysis data.

Chapter 3

Data & Methods

This chapter outlines the data and methodologies employed in Net-Zero scenario modelling, quantification of storage capacity, and identification of meteorological drivers behind storage depletion.

3.1 Scenario Modelling

This study examines Net-Zero scenarios that have not yet been realised, necessitating the construction of supply and demand time series representative of a 2050 power system. Bloomfield et al. (2022) created ERA5 reanalysis-based time series of wind and solar power capacity factors, as well as electricity demand, reflective of the 1950-2022 historical period. This data is publicly available online at the University of Reading Research Data Archive (Bloomfield et al., 2020a). This study utilises these weather-dependent time series and adapts them to be analysed within the context of the chosen Net-Zero energy systems.

3.1.1 Scenario Selection

Of the Net-Zero scenarios discussed in Section 2.2.1, three are selected to represent a plausible range of possible futures. The CREDS scenarios are excluded due to their significant divergence from those of the CCC and NG, particularly regarding offshore wind shares.

Johnson et al. (2023) highlights that NG's pathways exhibit the greatest demand reductions relative to 2020 compared to the CCC and CREDS. However, the study emphasises that NG's pathways omit key end-use sectors such as rail, aviation, and shipping. Given that rail demand is expected to increase in a Net-Zero scenario, and aviation and shipping have limited demand reduction potential, this omission may artificially underestimate the transport sector's demand requirements and, consequently, the overall pathway demand (Johnson et al., 2023). These pathways are therefore excluded from the analysis.

BEIS (2021) conducted an intermediate assessment on a subset of the CCC's scenarios (Headwinds, Balanced Pathway, and Widespread Innovation). These three were chosen to reflect an appropriate range of budget levels in order to meet the 2030 Paris Agreement's Nationally Determined Contribution and Net-Zero targets. The Balanced Pathway scenario was ultimately recommended as the preferred option by the assessment and the Devolved Administrations.

Given these considerations, subsequent analyses are based on the CCC's Headwinds, Balanced Pathway, and Widespread Innovation scenarios. This choice

is supported by the comprehensive and transparent data provided by the CCC, as well as the alignment of these scenarios with the UK government's broader policy objectives and budgetary constraints. Furthermore, the Balanced Pathway scenario is particularly desirable due to its built-in flexibility, intended to encompass a range of strategies to achieve Net-Zero.

All referenced data regarding the installed capacity, annual mean power, and other metrics relating to the scenarios are listed in Table 3.1, alongside their narrative description. Fig. B.1 in the Appendix B illustrates the sources of supply in the scenarios.

Figures	Unit	HW	BP	WI
Total demand	TWh	550	610	680
Total supply	TWh	655	775	941
VRE supply	TWh	427	427	623
Baseload supply	TWh	228	346	318
Solar capacity	GW	85	85	90
Onshore capacity	GW	25	30	35
Offshore capacity	GW	65	95	140
Peak demand	GW	114 (82)	101 (97)	113 (108)
Intra-annual variability	GW	N/A (36)	59 (46)	79 (50)

Narrative Descriptions

HW: No widespread behavioural shifts or innovations facilitate cost-reduction technologies. The pathway relies on large-scale hydrogen and CCS technologies to achieve Net-Zero. Electric vehicles account for 100 % sales of domestic vehicle sales by 2050, and there is significant use of hydrogen in HGVs. Heating is partially electrified, with 71 % of homes using hydrogen for heating. In manufacturing, blue hydrogen is more prevalent than electrification, resulting in lower electricity demand within power generation due to greater hydrogen use in homes.

Informed by the four other CCC pathways, this scenario makes moderate assumptions on consumer change and innovations, allowing for a range of approaches to achieving Net-Zero. Electric vehicles make up 100 % of sales in transport. 11 % of homes use hydrogen, with the rest relying on electrified heat networks. Manufacturing and construction depend on both hydrogen and electrification.

WI: Assumes successful cost-reduction technologies, enabling widespread electrification, greater energy efficiency, and more cost-effective greenhouse gas removal technologies. Again, there is 100 % sales of electric vehicles in transport. Ride-sharing, public transport, and active travel lead to significant demand reduction in transport. Consumer changes are similar to the CCC-HW scenario. Buildings are fully electrified, including heat networks. Manufacturing and construction are mostly electrified with some hydrogen use. This scenario features the highest deployment of renewables.

TABLE 3.1: Detailed overview of the three selected Net-Zero scenarios: Headwinds, Balanced Pathway, and Widespread Innovation. All figures are derived from the Committee on Climate Change (2020c), excluding those for peak demand and intra-annual variability, which are sourced from National Grid (2023b) and Ehsan and Preece (2022). Values in brackets indicate the actual values obtained through scaling, detailed in Fig. B.3 in Appendix B.

3.1.2 Solar

Bloomfield et al. (2022) models an hourly solar power capacity factor time series using gridded 2 m temperature and incoming surface solar irradiance, accounting for reductions in cell efficiency due to temperature deviations from standard test conditions. A national capacity factor is obtained by assuming a uniform capacity distribution across all grid boxes in the country, due to a lack of precise data on the distribution of solar generation locations. This is deemed acceptable within the context of this study given the relatively low penetration of solar power across the scenarios.

The solar power capacity factor time series is averaged over each day (00:00Z-23:59Z) and scaled by the installed solar capacity from each scenario to obtain a daily solar power time series.

3.1.3 Wind

Bloomfield et al. (2022) models an hourly wind capacity factor time series using gridded 100 m wind speeds, calculated from the zonal and meridional wind vectors, after a mean-bias correction was applied on a grid-point basis. These wind speeds are then converted into capacity factors using onshore and offshore power curves from National Grid (2019), shown in Fig. 3.1. The wind speeds are adjusted using a power-law profile to those expected at the UK average onshore (71 m) and offshore (92 m) hub heights.

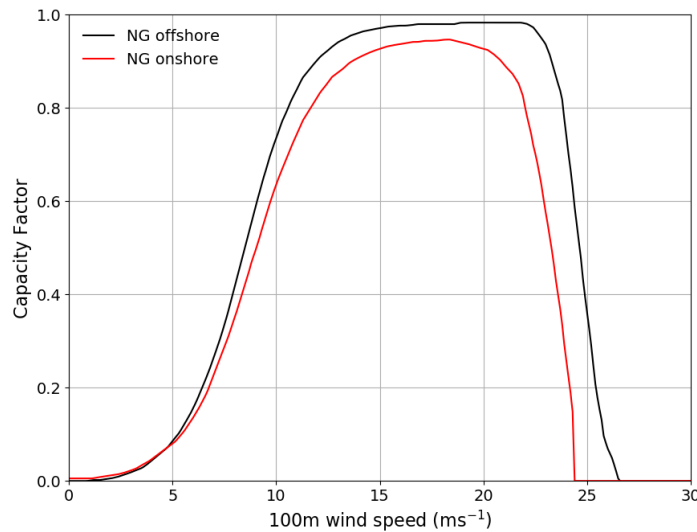


FIGURE 3.1: The wind power curves used by Bloomfield et al. (2022) to model the onshore and offshore wind power capacity factor time series, derived from the National Grid (2019) report.

A national capacity factor is obtained by weighting the gridded capacity factors according to the 2020 spatial distribution and installed capacity of wind turbines, sourced from thewindpower.net.

In this study, the onshore and offshore capacity factor time series are averaged over the period of one day and scaled multiplicatively by the installed onshore and offshore wind capacity from each scenario to obtain a daily onshore and offshore wind power time series.

3.1.4 Nuclear

The nuclear component of supply is modelled dynamically to respond to changes in supply and demand. The model generation typically ramps up when there is a supply deficit and ramps down when there is a daily surplus. The daily capacity factors for nuclear generation are set between 0.6 and 0.8, based on DESNZ and BEIS (2019) report of historical data from 1970-2015, which indicates that UK nuclear plants have generally operated within this range.

The following steps are used to create a daily nuclear time series:

- **Initialisation:** All days across the historical period are initially set to the minimum generation capacity factor of 0.6. This is then scaled multiplicatively by the installed capacity specified by the CCC for each scenario.
- **Annual Generation Correction:** Each year's annual nuclear generation is calculated. A scaling factor is applied to normalise the nuclear output to match the annual generation targets set by the CCC.
- **Daily Generation Correction:** The nuclear output is adjusted to ensure it stays within the daily minimum and maximum limits (set by the capacity factors and installed capacity).
- **Iterative Adjustment:** If the annual target is not met after the initial adjustment, an iterative adjustment is performed. The necessary net adjustment is calculated as the difference between the target and the current total generation. The nuclear output is then preferentially adjusted, adding equally to days in deficit first. If all deficits are addressed, any remaining adjustment is distributed across all days. This step is repeated until the annual target is met within 0.1 TWh.

3.1.5 Baseload

Generation excluding wind, solar, and nuclear are assumed to comprise a 'static baseload'. This includes sources like biomass CCS, gas CCS, unabated gas, geothermal, pumped hydro, batteries, and other renewables. The mean annual supply figures for each of these sources are aggregated for each scenario, and assumed to remain at that level throughout the time series.

3.1.6 Supply

The net supply time series, comprising aggregated wind, solar, nuclear, and baseload, is verified to match the mean annual supply specified for each scenario to within 1 %.

3.1.7 Demand

Bloomfield et al. (2022) modelled electricity demand in two steps. Firstly, a multiple linear regression model was created for the UK, with terms accounting for slow socio-economic changes over time and day-of-week effects. Additional terms for heating and cooling degree days quantified demand sensitivity to temperature, calculated as deviations from upper and lower temperature bounds.

Once the regression parameters were established, the second step applied the model across the entire historical period in the ERA5 dataset. The day-of-week terms were

set to Monday, and socio-economic changes were standardised to 2017 levels to isolate the weather effect on demand.

In this study, the demand data is adjusted to reflect changes in annual mean, seasonality, and variability due to the phasing out of gas in three scenarios. Ranges for peak demand and intra-annual variability in each scenario are used to construct the variability and seasonal cycle. The methods for obtaining these metrics are detailed in Appendix B.

The following steps are used to adjust the demand time series:

- **Seasonal Adjustment:** A cosine function is added to the demand to increase winter demand and decrease summer demand:

$$y_{\text{seasonal}}(t) = \delta_{\min} + (\delta_{\max} - \delta_{\min}) \cdot 0.5 (\cos(2\pi t/365) + 1), \quad (3.1)$$

where t indicates the day of the year (0-364), δ_{\min} is the minimum value of the seasonal adjustment, and δ_{\max} is the maximum value.

- **Vertical Shift:** A vertical shift is applied across the time series to align the current mean yearly demand with the desired mean yearly demand.
- **Manual Fine-Tuning:** The initial scaling factor and seasonal pattern are manually fine-tuned to ensure that the peak demand and intra-annual variability fall within their respective upper and lower bounds.

3.1.8 Supply-Net-Demand

Following the modelling of supply and demand time series, the instantaneous difference between the two, termed as supply-net-demand, is computed. This metric it serves as the input parameter into the storage model. Fig. 3.2 illustrates demand, supply, and supply-net-demand for the three scenarios over a one-year period.

Additionally, a 2020 scenario, constructed from 2020 data within the Balanced Pathway scenarios, is shown in black. This serves as a baseline to highlight the changes in seasonality and variability from the original data presented by Bloomfield et al. (2022) to the adaptations applied in this study. Note the differences in the y-axis scale across subplots.

The change in annual mean supply across scenarios is much more pronounced than demand. Demand is primarily shaped by the imposed seasonal cycle, with a winter surge and a summer reduction, compared to the shorter time scale variability introduced from the multiplicative scaling. The supply curve is predominantly influenced by short-term variability from the multiplicative scaling, with its natural seasonal pattern still apparent. The illustrated supply-net-demand time series is discussed in more detail in Chapter 4.

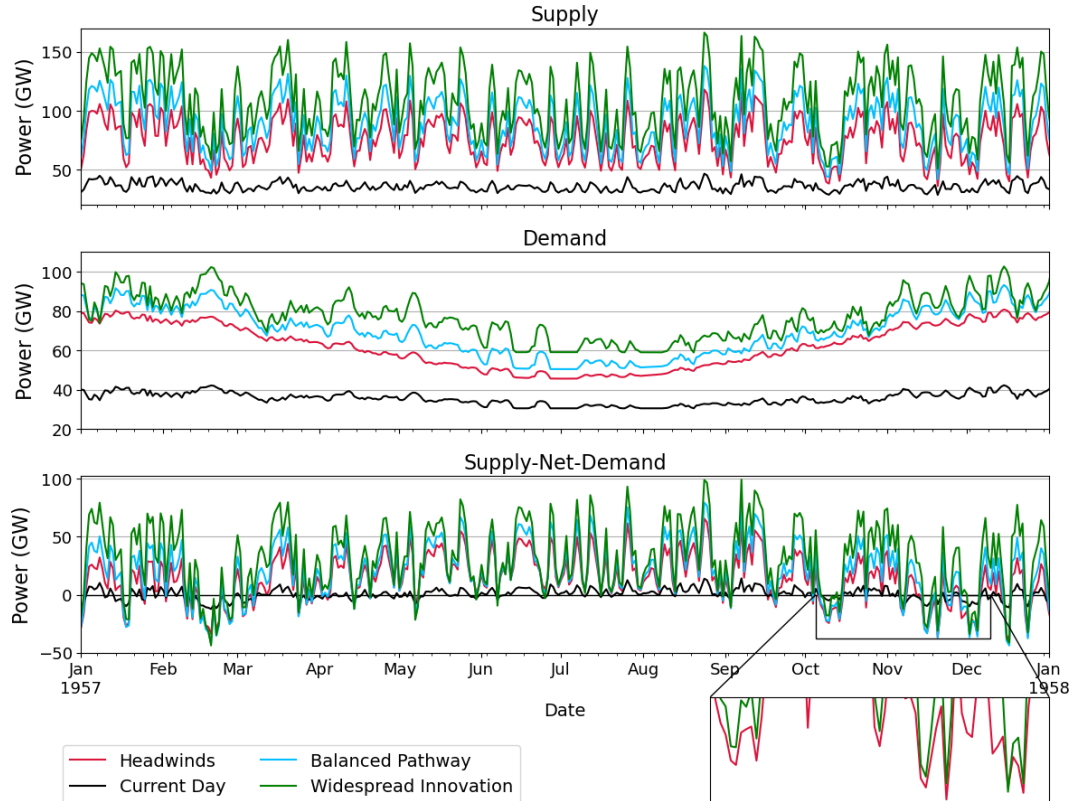


FIGURE 3.2: Supply, demand, and supply-net-demand profiles in GW for the three scenarios over a one-year period, shown alongside a 2020 Balanced Pathway profile. The supply-net-demand subplot illustrates that the Headwinds scenario experiences more pronounced and prolonged deficits compared to the Widespread Innovation scenario. The supply-net-demand profile is represented by the 5-day rolling mean; however, daily resolution exhibits greater variability.

3.2 Quantifying Storage

This section details the storage model and methodology used in Chapter 4 for quantifying the UK's required storage capacity and associated uncertainties under Net-Zero targets.

3.2.1 Storage Model

A bucket model simulates LDS dynamics using the instantaneous supply-net-demand as input. As shown in Fig. 3.3, the model stores surplus energy and withdraws energy during deficits. The input to the storage accounts for an electrolyser conversion efficiency and fuel cell conversion efficiency of 75 % and 55 %, respectively. A maximum conversion rate of 2352, applied after accounting for input efficiency losses, limits the rate at which input electricity can be converted to hydrogen. The model assumes no hydrogen leakage across any timescale. All parameters are consistent with those specified by The Royal Society in their report.

The model has an upper limit on storage capacity set at 200 TWh. Removing this cap leads to exponential growth in supply-net-demand and storage capacity.

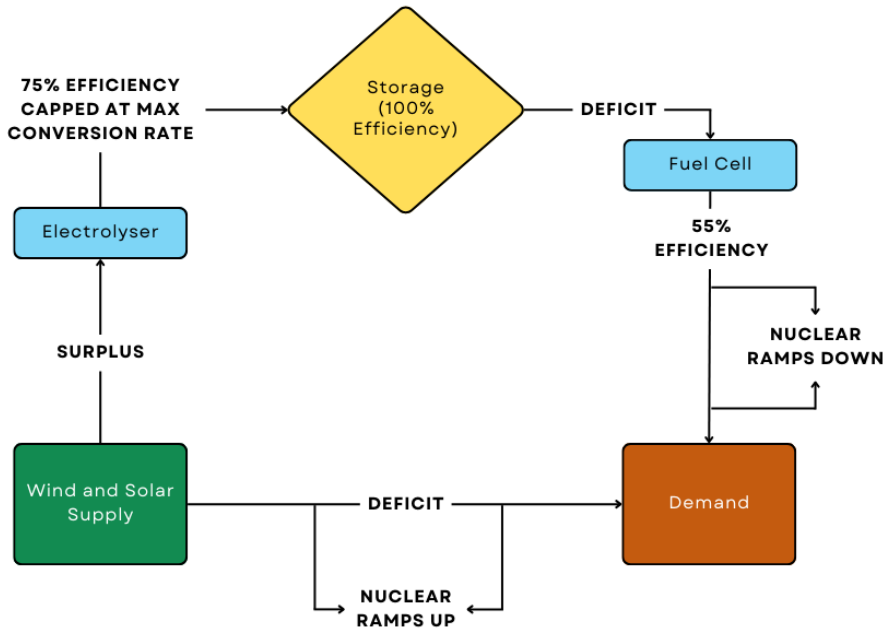


FIGURE 3.3: Flow chart of the storage model, beginning in the bottom left corner. The chart illustrates the process of converting surplus energy into storage after accounting for demand and efficiency losses, as well as the dynamic response of nuclear generation to ramp up and down accordingly.

Experimentation confirms that applying this limit does not affect the store's charge or discharge rate, or the storage capacity estimates. The capped model is preferred for its ease of calculation and superior computational efficiency in evaluating storage capacity.

3.2.2 Quantifying Storage Capacity

To quantify storage capacity, a robust method is needed to identify key regions in the storage model output. This requires defining storage depletion in a way that is applicable across all three Net-Zero scenarios.

A 'depletion peak' is defined as the lowest storage level each year, typically occurring between winter and spring. A 'depletion event' extends from this peak back to the last instance when storage was 'near full' for at least 20 consecutive days. Each depletion event is labelled by the year in which the peak occurs. Technical details of these definitions are provided in Appendix B.

'Required storage' denotes the capacity needed to address all energy deficits over a specified period, either the entire historical period or a single depletion event. It is calculated as the difference between the lowest instantaneous storage level and full capacity.

In addition to the traditional measure of storage capacity in TWh, this study employs an alternative metric from Dowling et al. (2020) for comparison with the literature. This metric, expressed in 'hours of mean demand,' is derived by resampling six-year periods starting from 1950, calculating the required storage capacity for each period,

and then dividing by the mean hourly demand. Given the daily data resolution, the mean hourly demand is approximated by dividing the mean daily demand by 24.

3.2.3 Quantifying Uncertainty

Monte Carlo Resampling

A Monte Carlo method is used to estimate uncertainty in the required storage capacity. The 72-year supply-net-demand dataset is resampled by drawing data for each month from all corresponding months in the dataset. February 29th is excluded to ensure a consistent 365-day year.

This monthly resampling generally preserves the annual depletion cycle of the storage from winter through spring. The method assumes that wind generation is independent from month to month, which is generally accurate except during DJF, when there is a stronger correlation between month-to-month NAO and wind generation.

Sampling repetition is permitted in the simulation. As each month from the historical dataset has an equal chance of being selected, this resampling maintains the probability distribution for rare events within any single month. However, this method does not necessarily preserve the likelihood of multiple rare events occurring in succession or within the same depletion cycle or year. The implications of these assumptions are discussed in Chapter 4.

In line with Muthén and Muthén (2002), which employed 10,000 permutations for stability, and Koehler et al. (2009), which recommended a similar number for accuracy and stability, this study performs 15,000 permutations for each Net-Zero scenario. The required storage capacity is recorded for each permutation.

Given this large sample size, the Central Limit Theorem ensures that the sampling distribution of the mean approximates a normal distribution. The upper bounds of the 99 % confidence intervals for storage capacity in each scenario are calculated using the standard error of the mean and the z-critical value corresponding to the 99 % confidence level.

A static nuclear baseload is used in this analysis to avoid excessive run-time due to the iterative nature of the dynamic baseload. Preliminary tests indicate that using a static baseload increases storage estimates by less than 2.5 %, and thus this simplification does not significantly affect the findings.

Simulating Successive Depletion

An alternative measure of uncertainty assesses the impact of a recurring event over consecutive years by repeating the 12-month period with the greatest depletion event (October 1958 to October 1959) either once or twice in the subsequent period. The required storage capacity is then calculated.

Varying Storage Efficiencies

The impact of varying storage system efficiencies on each Net-Zero scenario is assessed. Efficiency ranges are based on the projections from literature discussed in Section 2.3.4: 67 % to 74 % for electrolyser efficiency and 45 % to 55 % for generator

efficiency. Ten different efficiency values within these ranges were evaluated, and the corresponding storage requirements determined.

3.3 Identifying Meteorological Drivers

This section outlines the data and methods used in Chapter 5 for classifying the meteorological drivers that govern storage depletion.

3.3.1 Meteorological Data

The meteorological data for this study were obtained from the ERA5 reanalysis dataset, available online at the Copernicus Climate Store. Monthly mean values for four key meteorological variables were selected over the NAE region (40°W - 20°E , 20° - 80°N): 2 m temperature, 100 m mean wind speed, 100 m zonal and meridional wind components, 850 hPa geopotential, snowfall, and total precipitation. These variables were chosen to complement those used in constructing the scenario datasets from Bloomfield et al. (2022). Conversions were applied to adjust the units of temperature to $^{\circ}\text{C}$, and geopotential to geopotential height in m.

The mean wind speed was calculated from the zonal (u) and meridional (v) wind components ($\sqrt{u^2 + v^2}$). Unlike in the wind power time series, the ERA5 wind speeds were not bias-corrected. Consequently, these wind speeds may be underestimated for offshore regions and overestimated for onshore regions, as noted in research by Potisomporn et al. (2023) on 10 m ERA5 wind speeds over the UK.

Anomalies from climatology are calculated by subtracting the monthly average values, derived from the entire time series, from the corresponding meteorological data.

3.3.2 K-Means Clustering

A k-means clustering approach is employed to identify recurring synoptic-scale atmospheric patterns characterising depletion events throughout the Headwinds historical period. This widely used technique classifies atmospheric conditions by partitioning data into distinct clusters.

Given the monthly resolution of the meteorological data, only depletion events lasting at least 15 days within a single month were included in the clustering. This filtering ensures that the monthly mean is representative of 'depletion' weather, though it results in the exclusion of one event (1975) in Headwinds. Daily resolution data could mitigate this but would demand considerable storage and computational resources.

The clustering analysis utilises anomalies of 2 m temperature, 100 m mean wind speed, 100 m zonal and meridional wind components, and the mean wind speed. Variables such as snowfall and surface net solar radiation were excluded due to their negative impact on clustering performance. For each depletion event, composites of these anomalies were created, yielding mean anomalies for each variable during the event. These mean anomalies were then used for clustering.

The optimal number of clusters (k) was determined using the elbow method, which involves plotting the inertia (sum of squared distances) against various values of k

and selecting the k at the 'elbow' of the plot. As shown in Fig. 3.4, four clusters were identified as optimal for Headwinds.

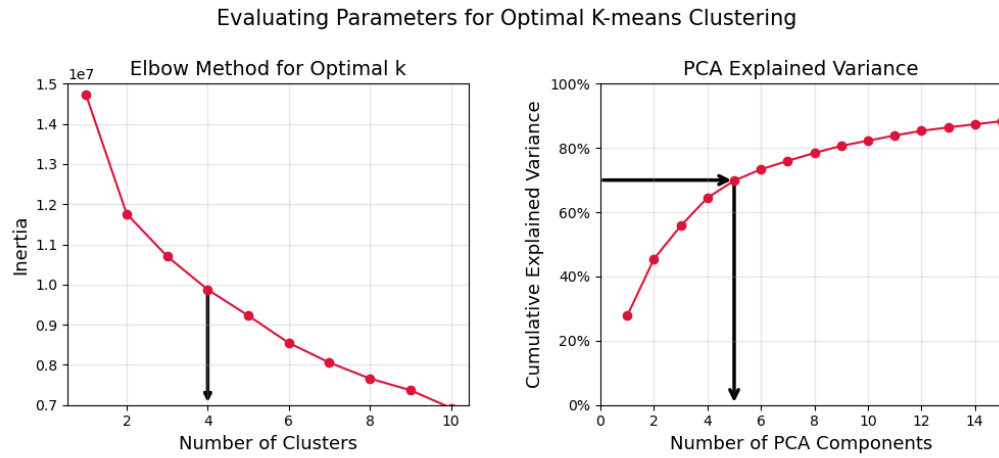


FIGURE 3.4: Evaluation of optimal k-means clustering parameters. The left plot uses the elbow method to determine the optimal number of clusters, with four clusters chosen. The right plot shows the cumulative explained variance from Principal Component Analysis, with six components selected to explain $\approx 75\%$ of the total variance.

Principal Component Analysis (PCA) was used to reduce the data's dimensionality by identifying the primary modes of variability. The explained variance is plotted against the number of components in Fig. 3.4. Grochowicz et al. (2024) selected principal components to capture 89 % of the variance in geopotential data. For this study, capturing approximately 75 % of the variance is deemed sufficient to focus on broad synoptic patterns while avoiding noise across the NAE region. Consequently, the first four principal components were selected.

K-means clustering was then performed on these components. The resulting silhouette score was calculated to measure the quality of the clustering, with a higher score indicating better-defined clusters. The silhouette score of 0.21 for Headwinds suggests overlapping clusters. However, for identifying broad atmospheric patterns, this score is reasonable.

K-means clustering was performed on these components. The silhouette score, which measures clustering quality on a scale from -1 to 1, was calculated. Higher silhouette scores are preferable; a score of 0.21 for Headwinds indicates some degree of overlap between clusters. However, despite this relatively low score, the clustering remains useful for identifying broad atmospheric patterns and provides valuable insights into the data.

3.3.3 Cluster Analysis

An analysis was conducted to compare the duration and required storage of the clustered depletion events. A non-parametric Mann-Whitney U test was used to evaluate the distributions of these variables across clusters, testing the null hypothesis that the distributions are identical ($\alpha = .05$). Given there are fewer than

25 samples per cluster and the distributions are skewed and non-normal but share similar shapes, this test is appropriate.

Chapter 4

Quantifying Storage

This chapter presents the results of modelling LDS under different Net-Zero energy scenarios, employing the methodologies outlined in Section 3.2. An overview is first provided of the constructed supply-net-demand time series, followed by an analysis of the storage model outputs. Additionally, three measures of uncertainty associated with these estimates are quantified.

4.1 Supply-Net-Demand

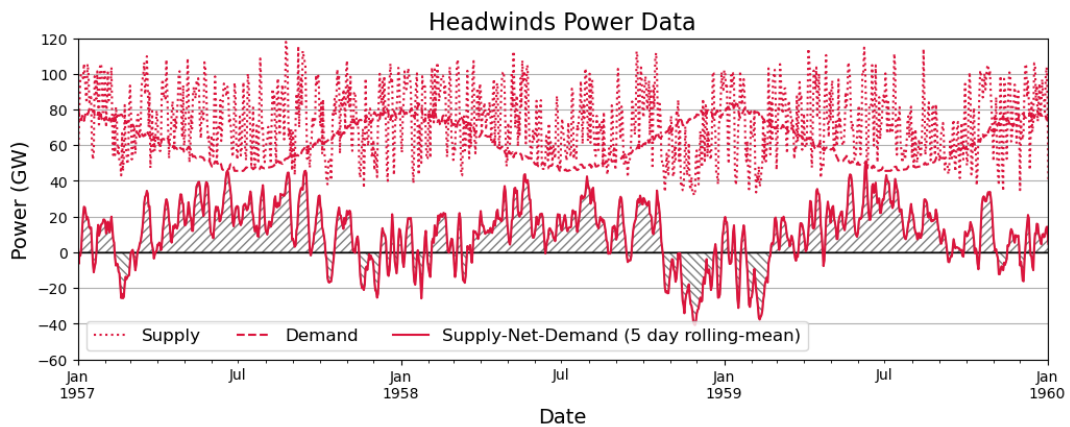


FIGURE 4.1: An example annual cycle of supply, demand, and supply-net-demand for Headwinds. The 5-day rolling mean is shown for supply-net-demand, highlighting greater variability on a daily timescale. Hatched regions above and below the x-axis indicate periods of energy surplus and deficit, respectively.

Fig. 4.1 illustrates the demand, supply, and supply-net-demand for the Headwinds scenario over a three-year period. The demand curve shows a marked seasonal pattern, with peaks during the winter and spring months due to increased heating requirements and troughs during the summer. This seasonal variation in demand is more pronounced than fluctuations over shorter timescales.

In contrast, supply generally peaks from autumn through winter, influenced by the southward displacement of the jet stream, and reaches its minimum during the summer. The supply curve is predominantly affected by short-term variability, with a secondary influence from seasonal patterns.

The supply-net-demand, which is the input for the storage model, reveals extended surplus periods when demand is low and/or supply is high (e.g., June-August), and deficit periods when demand is high and/or supply is low (e.g., February-March).

This chapter seeks to demonstrate that the magnitude, duration, and frequency of these deficit periods determine the need for storage, and that the magnitude and duration of the intervening surplus periods play a secondary role.

Further insights into the differences between scenarios can be gained by examining Fig. 3.2 and the supporting data provided in Table 4.1.

With increasing 'advancement' i.e. increasing electrification and RE deployment, the changes in the mean level and variance of supply become significantly more pronounced compared to changes in demand. Specifically, in the Headwinds scenario, the variance in supply is 2.8 times greater than that of demand, whereas, in the Widespread Innovation scenario, it becomes 5.3 times greater.

Variable	Headwinds (GW)	Balanced Pathway (GW)	Widespread Innovation (GW)
Supply Mean	67	80	104
Demand Mean	63	70	78
Supply-Net-Demand Mean	4	10	26
Supply Variance	357	550	847
Demand Variance	129	163	160
Supply-Net-Demand Variance	452	651	940

TABLE 4.1: Annual mean and variance figures for supply, demand, and supply-net-demand for the three Net-Zero scenarios.

Despite the highest variability in supply and demand observed in Widespread Innovation, its supply-net-demand consistently remains higher than in the other two scenarios, even during periods of high demand and low supply. This is illustrated by the supply-net-demand subplot in Fig. 3.2, which highlights that the Headwinds scenario is most prone to severe and prolonged deficits.

These findings indicate that the primary distinguishing factor between scenarios is the changes in the supply profile. Consequently, the level of wind power deployment is anticipated to be the main systematic driver of storage requirements, while the impact of demand electrification is more marginal.

4.2 Quantifying Storage Capacity

The storage time series for the three scenarios, spanning the 1950 to 2022 period, are shown in Fig. 4.2. The coloured highlighted regions in the subplot illustrate the duration of the depletion events according to their definition in Chapter 3.

A clear annual cycle is apparent, with storage typically depleting from winter to spring each year, reaching one local minimum peak. The greatest magnitude and most prolonged depletion events occur in the Headwinds scenario, followed by the Balanced Pathway and Widespread Innovation scenarios. The required storage

capacity for the entire historical period is 88 TWh, 79 TWh, and 49 TWh for these scenarios, respectively.

The results indicate that storage needs are greatest in scenarios with the lowest renewables deployment and least decarbonisation of gas in heating. This may appear counterintuitive, as LDS is rationalised in Chapter 1 as becoming more necessary with enhanced RE deployment and electrification. However, the lesser need for storage in more advanced scenarios can be attributed to the overall higher mean supply levels, which prevent prolonged deficits, as mentioned previously. While storage is most needed in the Headwinds scenario, this does not diminish its importance in the Widespread Innovation scenario; rather, it facilitates the high deployment of renewable energy within such a context.

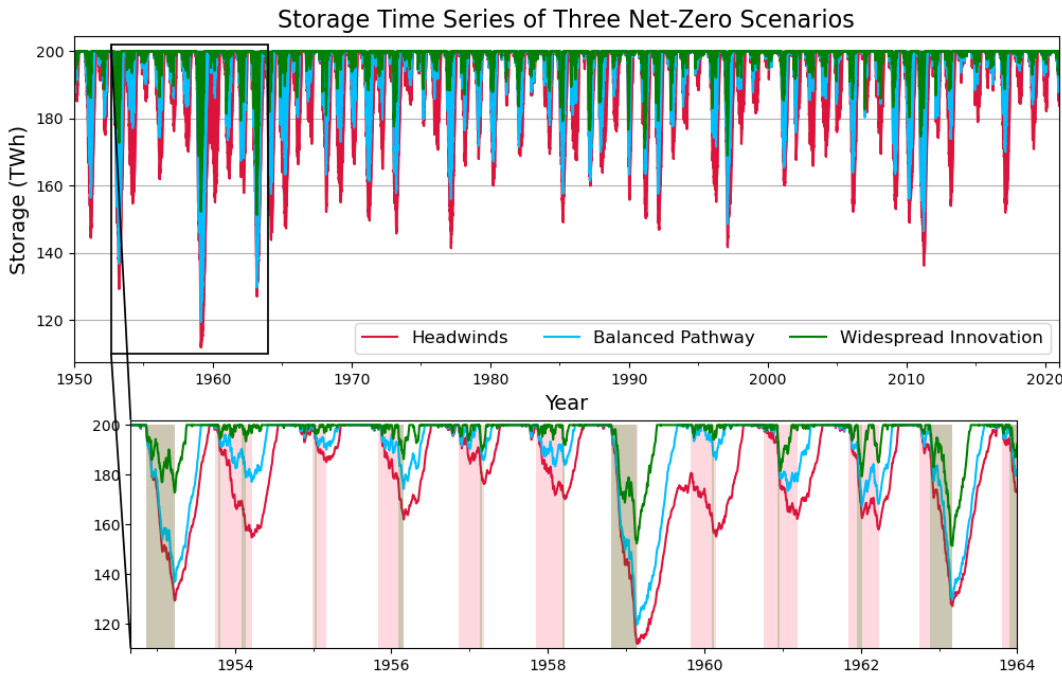


FIGURE 4.2: Modelled storage for the three scenarios from 1950-2022. The subplot provides a detailed view of the 1953-1964 period, which contains the three most prolonged and severe depletion events.

Furthermore, Fig. 4.3 illustrates the distribution of the dates corresponding to the start and end (peak) dates of the depletion events throughout the year. In the Headwinds scenario, depletion events typically start around October and peak in March, lasting an average of 93 days. In contrast, in the Widespread Innovation scenario, depletion events are more spread out from November to March but have a mean duration of 29 days.

This confirms that, on average, the Headwinds energy system leaves the LDS system more susceptible to periods of depletion over three times as long as in Widespread Innovation. This introduces the concept of 'resilience'—the ability to withstand prolonged periods of high demand and low supply before factoring in the capacity provided by LDS. This framework proves useful for characterising and comparing energy systems in this study.

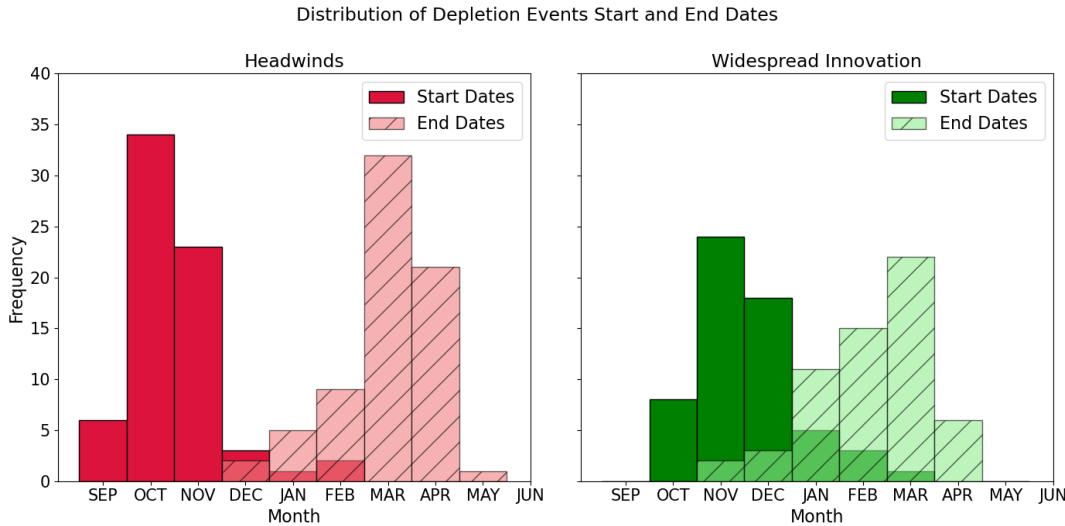


FIGURE 4.3: Distribution of the start and end (peak) dates of depletion events in the Headwinds and Widespread Innovation scenarios.

The lack of resilience in the Headwinds scenario is particularly evident in the 1959-1961 period, the only instance in the time series where Headwinds fails to recover to full capacity between two winter-spring events. In contrast, the other two scenarios demonstrate greater resilience, recovering more quickly and experiencing smaller magnitude depletions.

Additionally, the timing of these depletion events varies across the scenarios. The more advanced scenarios experience shorter depletion events within the longer periods seen in Headwinds. This suggests that the more advanced scenarios have higher thresholds for demand (lower temperatures) and lower thresholds for supply (lower wind) to which they are resilient. These shorter events tend to occur at any point within the Headwinds depletion periods, not just towards the peak in Headwinds. This threshold concept is shown to be true in Section 5.2.1.

For all scenarios, the top three depletion events occur within the 1952-1964 period, illustrated in subplot of Fig. 4.2. For Headwinds and Balanced Pathway, the top events is in 1959, and is distinguished from the second greatest event in 1963 by approximately 10 TWh. However, for Widespread Innovation, these two events have comparable storage requirements, with the 1963 event marginally being the most severe event.

The lesser relative reduction in the 1963 storage level in Widespread Innovation scenario is due to changes in meteorological drivers, which owe to the changes in the configuration of the energy systems themselves, and is discussed in Chapter 6. The Royal Society report's most severe event occurs in 2010, which forms the fourth greatest depletion event across this study's scenarios.

Consensus with the Literature

The different methodologies, scopes, and timeframes used among the literature discussed in Chapter 1 makes quantitative comparison challenging. However, several key points can be highlighted:

- **The Royal Society (2023a):** These three storage estimates are consistently lower than the 100 TWh base estimate reported by The Royal Society. This discrepancy can be partially attributed to the inclusion of a baseload supply in this study, which absorbs some of the energy deficits and thereby reduces the need for LDS. The contribution of nuclear generation is a much lesser factor due to its smaller share. Additionally, dynamic modelling of nuclear power only reduces capacity estimates by 2.5 % compared to static modelling.

Furthermore, had this study been limited to the 1980-2018 timeframe used by The Royal Society report, the storage estimates would reduce to 61 TWh, 52 TWh, and 30 TWh for the respective scenarios. This reflects a 1.7x change in Headwinds, and indicates that, given the apparent lower resilience of The Royal Society's model, extending its analysis to include this period would likely result in a storage requirement that exceeds the study's recommended 20 % contingency.

Accounting for the electrification and interannual variability of demand would likely further accentuate the differences between these two studies.

- **National Grid (2024):** The estimated 49 TWh of storage for the National Grid's 2024 Hydrogen Evolution Pathway aligns with that of the Widespread Innovation scenarios (49 TWh). Both scenarios feature substantial decarbonisation of gas and extensive offshore wind deployment, although Widespread Innovation leans more towards electrification than hydrogen. The National Grid's less advanced scenarios require less than 20 TWh of storage, whereas the less advanced scenarios in this study require more storage.

The discrepancy between the less advanced scenarios in this study and those of the National Grid may be due to the latter assuming a higher reliance on BECCS, geothermal energy, battery storage, and interconnections in those scenarios. These elements are also modelled dynamically rather than statically, potentially reducing the need for LDS.

Moreover, in contrast to the earlier comparison with The Royal Society report, where a shorter historical period increased the discrepancy between estimates, the National Grid's estimates, derived from a shorter historical period of weather and grid data, align more closely with this study's estimates for the shortened historical period.

- **Mouli-Castillo et al. (2021) & Kimpton et al. (2023):** Mouli-Castillo et al. (2021) estimated a storage requirement of 78 TWh for a scenario where only domestic heating is fully electrified. This estimate is comparable to those of the Headwinds (88 TWh) and particularly the Balanced Pathway (79 TWh) scenarios.

However, a direct comparison may be misleading. In the present study, electrification extends beyond domestic heating to include transport and industry, increasing the overall demand for storage. Additionally, in areas where electrification is not adopted, such as heating in buildings, hydrogen is integrated instead. This is especially the case in the Balanced Pathway scenario. These varying degrees of electrification and hydrogen adoption introduce complexities that challenge direct comparison.

The CCC notes that scenarios with higher hydrogen usage, like Balanced Pathway, generally require more extensive LDS (CCC, 2023). Given this

and their greater overall electrification, it is expected that Balanced Pathway and Widespread Innovation would have higher storage estimates than Mouli-Castillo et al. (2021), while Headwinds might have a lower estimate. It is also expected that this study's estimate would fall below the 150 TWh estimated by Kimpton et al. (2023) for the full integration of hydrogen into the gas network. The findings of this study align with both of these expectations.

- **Dowling et al. (2020):** Dowling et al. (2020) estimated a median need of ~ 710 demand hours of storage capacity for the United States when using a simulation lengths of 6 years across the 1980-2016 timeframe, as shown in Fig. 2.2. The present study's LDS capacity estimates were recalculated using the same methodology and 6-year simulation period, with results shown in Fig. 4.4.

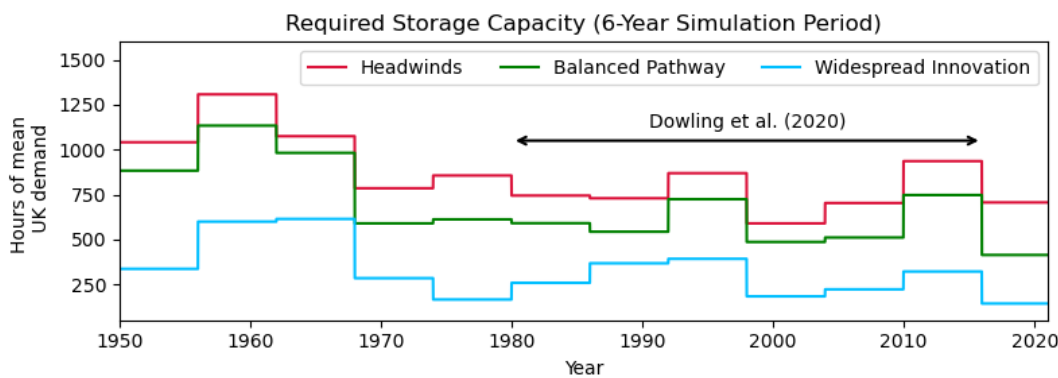


FIGURE 4.4: LDS capacity estimates from a 6-year simulation period using the 72-year historical dataset, expressed in hours of mean demand. This analysis follows the method of Dowling et al. (2020), shown in Fig. 2.2, with the shorter time period used in their study also indicated for comparison.

This approach results in median storage capacity estimates of 856, 611, and 321 hours of mean UK demand for Headwinds, Balanced Pathway, and Widespread Innovation, respectively. The Balanced Pathway is particularly close with only a 14 % difference from that of Dowling et al. (2020).

Had this study been limited to the same time period as Dowling et al. (2020), the storage estimates would have been 730, 543, and 260 demand hours, bringing the Widespread Innovation estimate more in line with the estimates of Dowling et al. (2020). This shift can be attributed to the 1950s–1960s period, which features a clustering of severe depletion events.

Additionally, the discrepancy between the two studies can be attributed to different modelling methods. Dowling et al. (2020)'s study, based on a US energy system, optimises storage capacity to minimise system costs in a 2040–2050 future, rather than explicitly modelling Net-Zero energy systems. As a least-cost optimisation, however, it may have preferentially modelled a high-wind power electricity system due to its lower costs. This could explain why the study's estimate is most similar to the high-wind power scenario of Widespread Innovation.

- **CCC (2023):** Counterintuitively, among the literature reviewed, this study shows the greatest deviation from the CCC's estimates of 7 TWh to 12 TWh of storage for the same scenarios. Unfortunately, a detailed comparison is limited due to the lack of detailed documentation on its storage modelling methodology.

This study's initial estimates encroach on the higher-end estimates found in the literature. When accounting for the different methodologies and time periods used, the estimates are found to lie above those from comprehensive, system-wide studies such as National Grid (2024) and Committee on Climate Change (2023). They are also found to lie below those from more focused studies on LDS and gas heating decarbonisation, such as The Royal Society (2023a) and Kimpton et al. (2023).

Overall, this study's findings are consistent with the existing literature. An important observation from this analysis is that other studies examining similar wind-dominated energy systems could potentially return higher storage estimates if they extend their datasets to include the high-electricity demand 1950-1960s periods.

4.3 Quantifying Uncertainty

This section examines two primary sources of uncertainty in quantifying storage capacity: the limited availability of historical weather data and the unpredictable future advancements in storage technology efficiencies.

4.3.1 Weather Uncertainty

Monte Carlo Resampling

A Monte Carlo simulation was conducted for each scenario, as detailed in Section 3.2.3, resulting in the distribution of required storage for 15,000 permutations, illustrated in Fig. 4.5. The dashed horizontal lines represent the storage capacity estimates from the previous section.

The absolute maximum values of the distribution indicate a need for contingency storage exceeding 20 TWh. However, these extreme values are unlikely to be realistically considered, as storage is built to accommodate a reasonable range of potential extreme events rather than a single probabilistic permutation.

Attention is thus focused on the upper bound of the 99 confidence intervals, which show that the storage capacity requirements for the Headwinds, Balanced Pathway, and Widespread Innovation scenarios do not exceed 73 TWh, 62 TWh, and 37 TWh, respectively, in 99 of simulations. These values are below the estimates determined in the previous section, suggesting that no additional contingency is required for any of the scenarios.

The substantial 10 % to 20 % difference between the previous base estimate and the confidence level arises from the implicit assumption from the sampling methodology of independence between consecutive supply and demand months. This may underestimate the likelihood of consecutive months experiencing rare weather conditions, leading to lower storage requirements. For instance, if January experiences a low-supply, high-demand event followed by a recovery period, and February is independently resampled and also starts with a similar event, the recovery period at the end of January reduces the overall storage requirement.

In contrast, the original historical sequence might result in a more sustained high-demand period without such an intervening recovery phase, requiring higher storage.

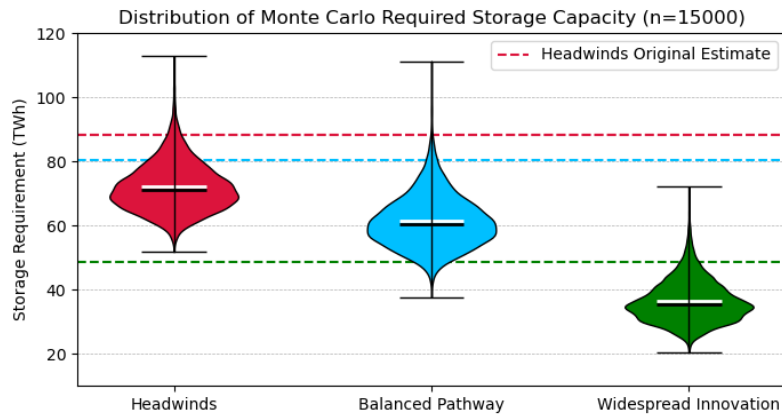


FIGURE 4.5: Distribution of required storage capacity estimates for each Net-Zero scenario using the Monte Carlo resampling method with 15,000 permutations. Dashed lines represent the base capacity estimate from Section 4.2, before resampling. White and black markers indicate the mean and median of the distribution, respectively.

This highlights the importance of preserving the month-to-month DJFM correlation between the NAO and wind speeds and temperature. Further analysis revealed significant, moderate Pearson correlation coefficients between the monthly mean DJFM NAO index anomalies and both demand anomalies (-0.55) and supply anomalies (0.42) for the Headwinds scenario. Future studies should consider this relationship, modifying the Monte Carlo method to yield more insightful results.

Simulating Successive Depletion

Considering the limitations of the previously discussed Monte Carlo method, a more direct approach to measuring the uncertainty is implemented. This method assumes the October-September months associated with the worst depletion event, the 1959 event, reoccur in the following year for one test and in two successive years for another test.

The results indicate a required storage capacity of 106 TWh (+20 %) and 124 TWh (+41 %) for two and three repetitions, respectively, for the Headwinds scenario, and no contingency is required for the other two scenarios. This is attributed to Headwinds' lack of resilience; its relatively lower supply levels prevent recovery to full capacity after each winter, leading to progressively lower depletion levels with each repeated cycle.

This successive-1959 approach essentially represents a single possible permutation of a Monte Carlo resampling conducted using whole-year blocks instead of months. This method would preserve the DJFM correlations within an individual annual cycle of the store, providing a more robust measure of uncertainty.

4.3.2 Efficiency Uncertainty

A sensitivity analysis of required storage capacity was conducted with varying input and output efficiencies, ranging from lower-end combinations to the high-end efficiencies used in The Royal Society report. The results are shown in Fig. C.1 in Appendix C.

When the efficiencies were changed from the high-end pair used in the base estimates across the tested range to the lowest-end pair, the required storage capacity increased by 20 TWh to 22 TWh across the three scenarios.

4.3.3 Implications for Quantifying Storage Capacity

The findings from all three methods of quantifying uncertainty are discussed here. Regarding the uncertainty due to finite data, it seems unlikely that a scenario with lower societal change and less adoption of renewables would aim to build LDS capacity to withstand three consecutive 'bad' years. Therefore, an additional contingency of 18 TWh (20 % from the base estimate) is suggested for Headwinds only.

Given that the Widespread Innovation and Balanced Pathway scenarios involve higher levels of technological advancements, it is less plausible they would operate at lower-end efficiencies. For Headwinds, it is assumed that efficiencies are at the middle-to-lower end for both input and output conversions, necessitating an additional 17 TWh of storage. For Balanced Pathway, efficiencies are assumed to be at the middle-to-high end, suggesting an additional contingency of 6 TWh. Widespread Innovation is assumed to adopt the upper-end efficiencies used in the base estimates, so no additional storage requirement is needed.

The combined impact of these two uncertainties, calculated by adding their respective contributions, results in storage capacity estimates of 123 TWh for Headwinds, 85 TWh for Balanced Pathway, and 49 TWh for Widespread Innovation. However, the aggregate impact could ideally be more accurately determined using the year-block Monte Carlo resampling method, applied with the assumed efficiencies for each scenario, to provide storage requirements based on the resulting 99 % confidence level.

These final estimates have two implications:

- The impact of efficiency-induced uncertainty is of comparable magnitude to the finite data-based uncertainty for Headwinds. Furthermore, the lack of resilience and technological development in this scenario drives its need for storage to be 2.5 times greater than for the Widespread Innovation scenario.
- These estimates broadly still lie within the upper and lower boundaries of the literature discussed in Section 4.2. Of the literature reviewed, only The Royal Society (2023a) explicitly accounts for the finite data-based uncertainty. The report recommends 23 TWh (20 %) for its Headwinds-akin scenario. This closely aligns with the 18 TWh suggested by the present study for Headwinds.

Despite the flawed application of the Monte Carlo method, this study has made progress in incorporating uncertainties into the quantification of LDS capacity, an area not extensively addressed in the literature.

4.4 Further Comparison with the Literature

The Royal Society's work on quantifying LDS capacity serves as a key reference in this study. Comparing the methodologies adopted by the two studies enables potential improvements for future Net-Zero and LDS modelling to be identified. To facilitate a clearer comparison, this study recalculates its storage model output using the supply and demand parameters from The Royal Society's scenario, detailed in Chapter 1. In this configuration, there is no baseload, no electrification of demand, and the demand for each year is modelled using 2018 demand data. The resulting storage time series is shown in Fig. 4.6 for the entire 1950-2022 period, alongside an excerpt of the 1980-2016 period used in The Royal Society report.

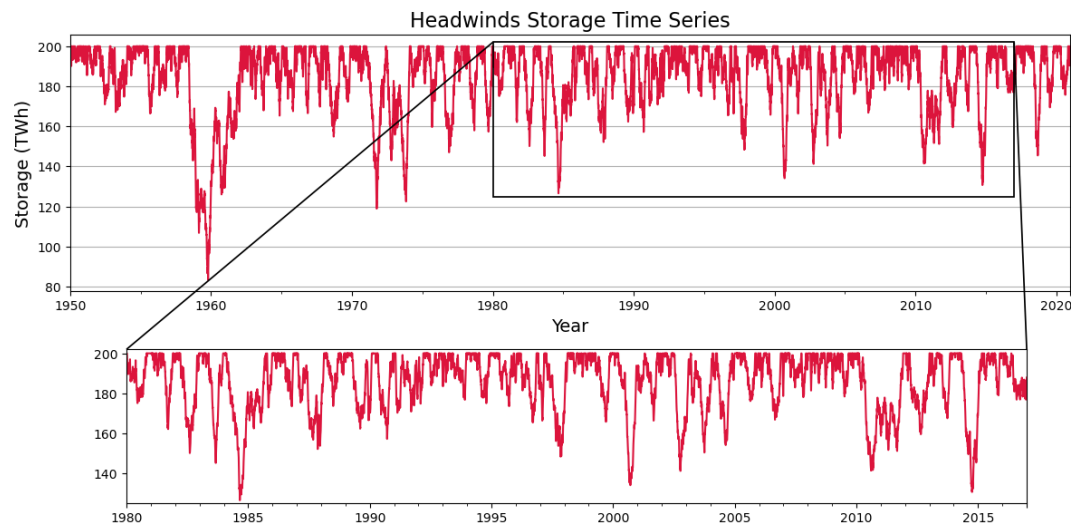


FIGURE 4.6: Modelled storage from 1950-2022 using data from this study and a methodology aligned with that of The Royal Society's report. The subplot provides a detailed view of the 1980-2016 period, from which The Royal Society derived its capacity estimates.

Both figures show alignment in general periods of depletion but with differing relative magnitudes of depletion and recovery. Considering that previous findings indicate the majority of variance in supply-net-demand can be attributed to wind power, it is suggested that these differences may lie in the modelling of wind supply. Investigating the exact origins of these differences is beyond the scope of this study.

Additional insights emerge when considering the role of electrification and interannual variability of demand in LDS modelling. If the full demand profile is incorporated instead of the repeated 2018 demand profile, this results in a minimal increase in required storage capacity of 6 TWh. This finding aligns with The Royal Society's post-publication analysis, which found a capacity increase of less than 10% (The Royal Society, 2023b).

However, in the original energy system used throughout Section 4.2, the required storage capacity increases by up to 6%, 16%, and 45%, for the respective scenarios, relative to when the 2018 demand is repeated in the same configuration.

This suggests that using the 2018 demand profile repeatedly was acceptable within the context of The Royal Society's report and its contingency. However, in the present study, such an approach would lead to a significant underestimation of

the storage needed, even exceeding the capacity accounted for by the suggested contingency.

These findings lead to three interconnected insights, which collectively influence both the modelling of LDS systems and the interpretation of their results in the literature:

- **Modelling Complexity:** Comparing capacity estimates from literature is challenging due to the compounding effects of assumptions in both the modelling of supply and demand profiles, as well as the Net-Zero energy system in which they are contextualised. These assumptions may be reasonable in one study but not transferable to another. Their inclusion must be balanced to avoid overestimating or underestimating storage capacity.
- **Resilience:** This study's energy system has shown to be more resilient than the one tested in The Royal Society paper, partly due to its supporting non-RE baseload. This highlights the trade-offs between rapid decarbonisation, such as extensive wind deployment, and the need for supportive measures like nuclear to maintain system resilience. This concept is further explored in Chapter 5.
- **Meteorological Drivers:** The meteorological conditions with the most severe impacts can differ between systems. For example, The Royal Society report's energy system may be vulnerable to decadal period of low-solar due to its significant 20 % solar share. This underscores the importance of diversifying energy sources to mitigate risks associated with specific weather conditions.

It is also crucial to distinguish between apparent differences in meteorological drivers caused by modelling assumptions and the actual drivers that would prevail without such assumptions.

Chapter 5

Identifying Meteorological Drivers

This chapter analyses the meteorological drivers of storage depletion across different Net-Zero energy scenarios, following the methodologies outlined in Section 3.3. The analysis is presented in three parts: firstly, a case study examines a single depletion event within the Headwinds scenario; secondly, a comparative study explores the differences in meteorological drivers between the Headwinds and Widespread Innovation scenarios; and finally, clustering techniques are used to identify the broader drivers throughout the historical period of the Headwinds scenario.

5.1 Case Study: Most Severe Depletion Event

The winter of 1958 to the spring of 1959 coincides with the most severe storage depletion event in terms of magnitude and duration in two of the three Net-Zero scenarios considered. This section aims to identify the meteorological drivers of this event using the Headwinds data, referring to the findings of Namias (1964), which identifies this period for its persistent blocking activity.

Fig. 5.1 (top) illustrates the anomalies from climatology of power variables including solar, onshore wind, and offshore wind power, as well as demand and supply-net-demand. The plot spans from the onset of the depletion event through part of the subsequent recovery. In the storage time series (bottom), the 1959 depletion event is evident in three distinct periods of storage discharge: November and December 1958, and January 1959. The monthly mean fields of geopotential, temperature, and wind speed anomalies for these periods are shown in Fig. 5.2.

5.1.1 Stage One: November 1958

In November, an east-to-west temperature gradient of ~ 2 $^{\circ}\text{C}$ between Ship Charlie and Ship India strengthened the southerly component of the thermal wind in the lower troposphere in the surrounding regions. According to Namias (1964), this enhanced northward transport of warm air contributed to the formation of a ridge farther east over Scandinavia. This is illustrated in Fig. 5.2, which shows an extensive ridge centered over Scotland and the Scandinavian Peninsula.

A ridge in the upper atmosphere leads to stable weather and less cloud cover, increasing solar radiation. The enhanced northward transport and warming increase the SST gradient, likely creating a positive feedback mechanism that reinforces the ridge formation.

Namias (1964) also proposed another underlying mechanism that favours ridge formation. Reduced spring-autumn precipitation resulted in a lack of winter snow

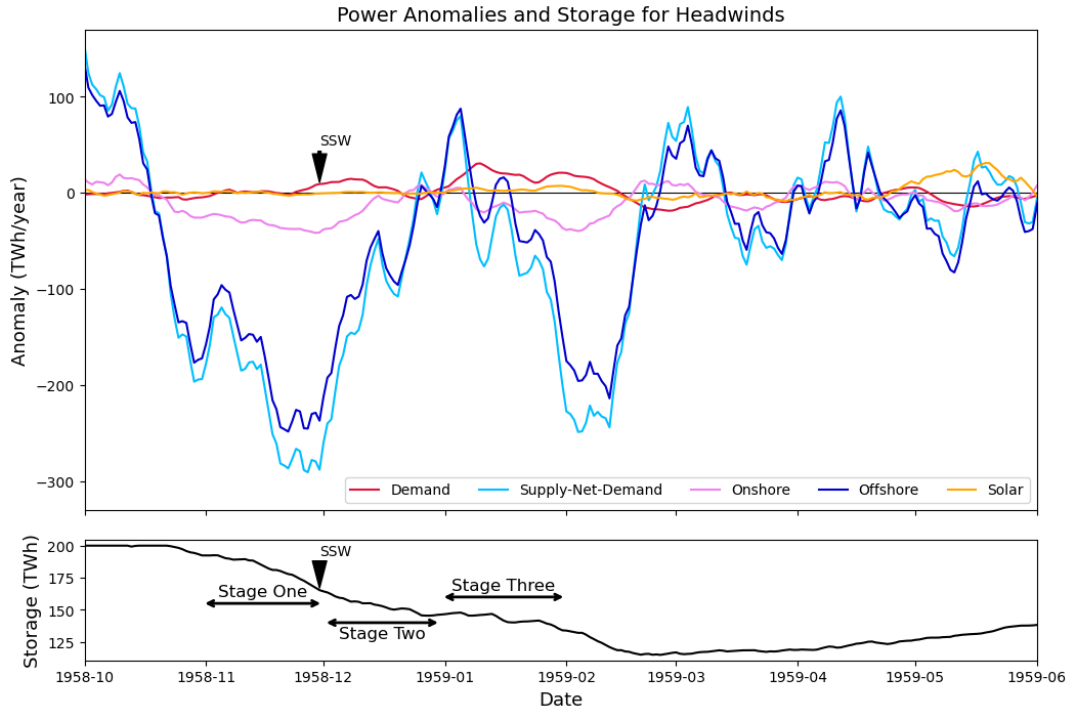


FIGURE 5.1: Time series of power variable anomalies from climatology (top) and storage time series (bottom) for the 1959 depletion event and subsequent recovery period. The 15-day rolling mean is shown for the power anomalies. The timing of an SSW event and the three stages of the depletion event are marked.

cover, increasing the thermal contrast between the Scandinavian Peninsula and the Atlantic and Baltic Seas. This created favourable conditions for the formation of upper-level anticyclones above the peninsula. Fig. 5.3 shows the mean anomaly fields of temperature, total precipitation, and snowfall from the prior spring-autumn period, confirming below-normal precipitation and snowfall, and above-normal temperatures, which contrast with below-normal Baltic Sea temperatures. This snow-ridge formation mechanism is suggested as an initiating factor for the 1959 depletion event.

In the GWL classification system, the resulting blocking system would be equivalent to the HFA (Scandinavian High, ridge over Central Europe) and/or a High over British Isles GWL regime. This regime caused widespread reductions in climatological southerly and westerly wind speeds over much of the UK and Europe (meridional winds are shown in Fig.D.1 in Appendix D). Consequently, this led to below-normal temperatures throughout western Europe, while Scotland experienced above-normal temperatures. The reduced wind speeds likely resulted in lower wind power generation, while the colder temperatures increased electricity demand for heating. Together, these factors contributed to significant storage depletion during the event.

The resulting blocking system corresponds to both 'Scandinavian High, ridge over Central Europe' and a 'High over British Isles' GWL regimes. This caused widespread reductions in climatological southerly and westerly wind speeds over much of the UK and Europe (meridional winds are shown in Fig.D.1 in Appendix D).

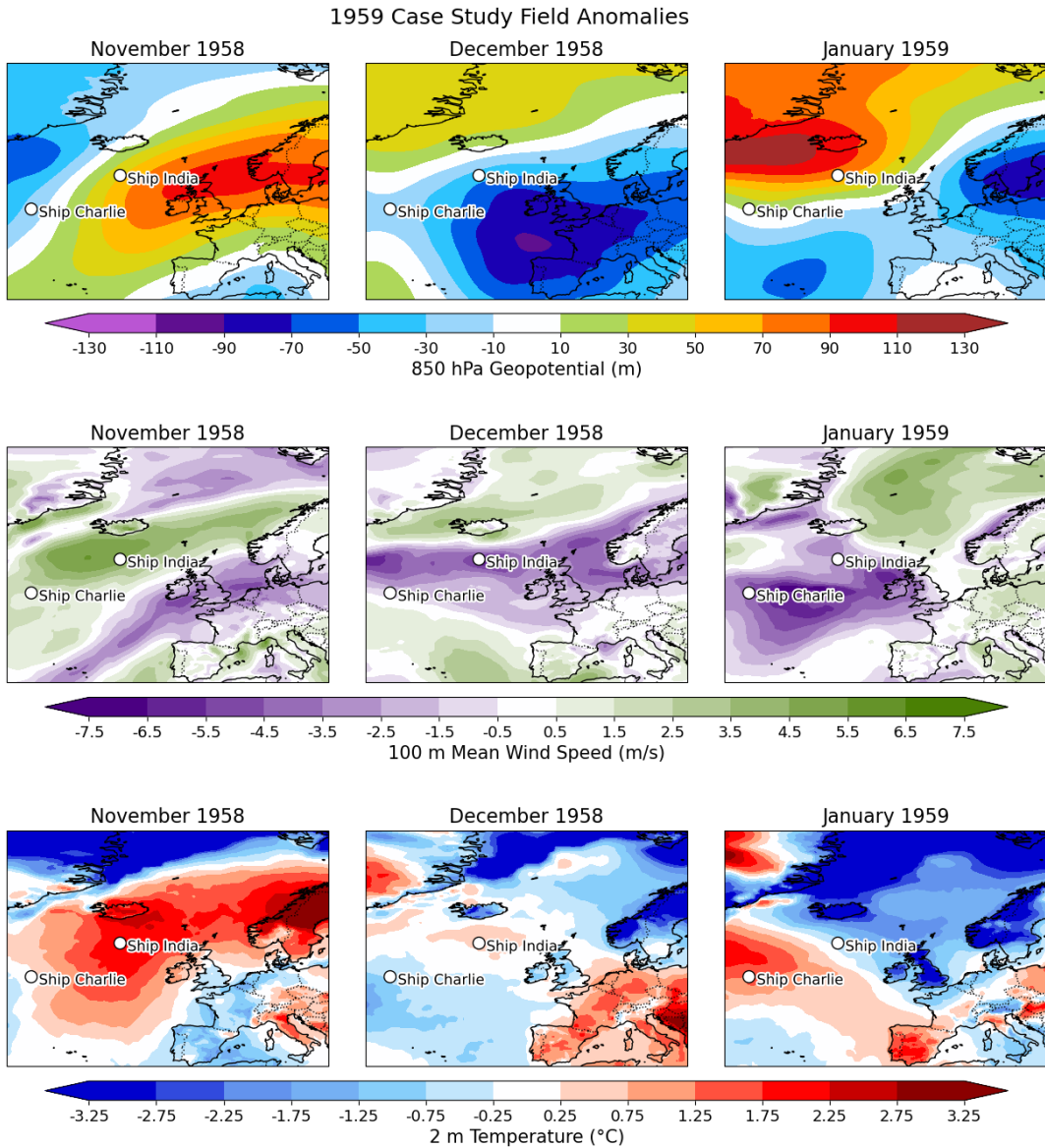


FIGURE 5.2: Monthly mean meteorological field anomalies from climatology for the 1959 depletion event case study. The left column shows anomalies for Stage One (November 1958), the middle column for Stage Two (December 1958), and the right column for Stage Three (January 1959). The locations of Ship Charlie and Ship India, referenced by Namias (1964), are marked.

Consequently, this led to below-normal temperatures throughout western Europe, while Scotland experienced above-normal temperatures. The reduced wind speeds would correspond to lower wind power generation, while the colder temperatures increased electricity demand for heating.

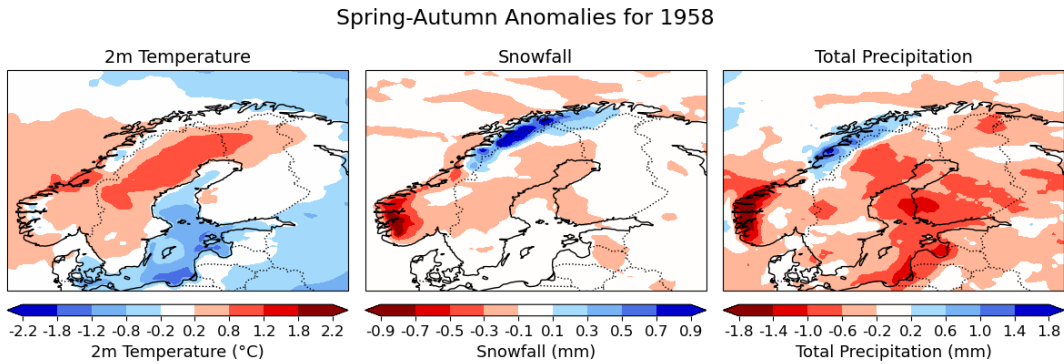


FIGURE 5.3: Mean meteorological anomalies for Spring-Autumn 1958, showing the monthly mean 2m temperature, snowfall, and total precipitation. The data indicate above-normal temperatures and precipitation, leading to below-normal snowfall across the Scandinavian Peninsula.

5.1.2 Stage Two: December 1958

In December, the blocking situation transitioned into a widespread trough centered in the Bay of Biscay, extending across Northern and Southern Europe, and much of the North Atlantic. Simultaneously, a weak ridge began forming over Greenland. This pattern aligns with the 'Trough over Western Europe' (TRM) GWL regime.

In December, the blocking pattern transitioned into a longitudinally and latitudinally trough centered in the Bay of Biscay. A weak ridge began to form over Greenland. This pattern aligns with the 'Trough over Western Europe' (TRM) GWL regime.

This change in the mean synoptic pattern is suggested to be attributed to a SSW event, along with general atmosphere-ocean thermal dynamics. According to the NOAA Sudden Stratospheric Warming Compendium dataset (NOAA CSL Chemistry & Climate Processes, 2024), an SSW event was recorded on 30 November 1958, in the NCEP-NCAR reanalysis product. This SSW event may have weakened the polar vortex, allowing the jet stream to meander more than usual, leading to a southward shift of the Icelandic low followed by the formation of a new, deep trough. This shift is consistent with the colder air masses moving southward, as evidenced by the dissipation of the previous positive temperature anomalies in Fig. 5.2.

As evidenced in Chapter 2, SSWs can increase the likelihood of transitioning into NAO- conditions. This aligns with the formation of a Greenland blocking system.

The dissipation of the ridge over the Scandinavian Peninsula may also be attributed to the lack of insulating snow cover. This could have led to more rapid surface cooling as winter progressed, decreasing the pressure gradient with the surrounding regions. With a weakened ridge, atmospheric circulation became more conducive to the development and persistence of low-pressure systems.

Fig. 5.1 shows that the wind speeds across the UK, although still lower-than-normal on average for the month, were higher than in the previous month, and the same trend was observed in temperature. This is reflected in the slightly lower rate of discharge in the storage.

5.1.3 Stage Three: January 1959

In January, the trough appears to split into two smaller troughs, positioned over the Scandinavian Peninsula and the Azores. As the effects of the SSW propagate and evolve, the ridge over Greenland matures. This pattern aligns with the 'Icelandic high, ridge over Central Europe' (HNA) GWL regime, or a broadly negative NAO regime. Similar to the 'Beast from the East' in 2018, it is likely that the SSW primed the NAO transition into a negative phase from early December through January.

In Fig. 5.2, there is an indication of another ridge southeast of the Mediterranean, extending beyond the visible area of the image. The resulting quadripole pressure system has compounding effects on the UK. The Scandinavian trough induces a cyclonic flow, while the Icelandic ridge creates an anticyclonic flow, reinforcing a strong northerly wind component over the UK. Additionally, the Scandinavian and Azores troughs introduce opposing cyclonic flows, creating a convergence zone over the UK. This convergence forces air upward and reduces horizontal wind speeds near the surface.

The drop in temperature is also consistent with the occurrence of the SSW. Fig. 5.1 shows that the demand anomaly is mostly normal but starts increasing prior to the SSW, with above-normal demand peaking approximately 1.5 months after the event. This aligns with findings by King et al. (2019), where cold extremes (and therefore high demand) tend to be strongest 1-2 months after an SSW.

A study by Mockert et al. (2023) on Dunkelflauten found that Greenland Blocking, characterised by a quadripole pressure system, resulted in prolonged cold and less windy conditions, increasing electricity demand and reducing renewable energy output. These findings support this study, highlighting Greenland Blocking as a key contributor to the most prolonged and severe depletion event in the historical period.

5.1.4 Implications

The 1959 depletion event can be summarised over the three-month period as follows: Wind speeds reached their lowest point between Stage One and Stage Two, while temperatures progressively declined, reaching their lowest in Stage Three. This mismatch between the worst wind conditions and peak demand led to prolonged stress on the energy system, preventing storage recovery and necessitating deeper storage use.

This period was characterised by three regimes: a Scandinavian blocking regime, a trough over western Europe, and an NAO-tripole regime. The drivers of these regimes, and therefore the drivers of the storage depletion, are attributed to a combination of ridge formation feedbacks with SSTs, snow cover, and the occurrence of SSWs. The literature suggests that Scandinavian blocking may have preconditioned the atmosphere for the SSW events, which in turn favoured the transition to an NAO- regime.

Understanding the drivers behind the most significant event in these systems is essential for predicting how similar meteorological conditions could affect other Net-Zero energy systems. Notably, the 1959 event marks the only instance where the Headwinds scenario fails to recover, and it also precedes the longest recovery period for all scenarios.

This suggests that a Headwinds-akin scenario, characterised by a higher degree of electrification but lacking a corresponding increase in supply, could be particularly vulnerable to similar meteorological conditions. In such a scenario, insufficient renewable supply and the lack of large-scale LDS implementation could further expose the energy system to risk. This underscores the importance of a balanced approach to the transition to Net-Zero, highlighting the risk of accelerating decarbonisation of one aspect of the energy system, such as heating, without ensuring adequate sustainable levels of supply to support it.

5.2 **Changing Drivers Across Scenarios**

This section analyses the meteorological conditions that become apparent when comparing the least and most advanced Net-Zero scenarios: Headwinds and Widespread Innovation.

5.2.1 **Changing Surface Conditions**

Composite anomaly fields of various variables during depletion events throughout the historical period are examined. The purpose of this is to establish the overall synoptic conditions driving the need for LDS. These composites are shown in Fig. 5.4.

Both scenarios reveal a clear 'High Scandinavia-Iceland, ridge/trough over Central Europe' (HNFZ/HNFA) regime. These two regimes are identified in Brayshaw et al. (2012) as being associated with colder, windier conditions across the UK. Notably, the HNFZ type accounts for a significant portion of the extreme peak demand days in the UK between 1987 and 2006, including the four highest peak demand days.

In the Widespread Innovation scenario, the ridge is less than 10 m higher than in the Headwinds scenario. The zonal wind anomaly is also more easterly, indicating a more weakened climatological westerly. This reduced influence of mild maritime air masses results in temperature anomalies being lower by about $\sim 0.5^{\circ}\text{C}$ in Widespread Innovation.

This scenario also features higher direct solar radiation (not shown), though this difference is spatially inconsistent across the UK and likely negligible due to the low installed solar power in both scenarios. Subject to feasibility, increasing the deployment of solar power could potentially boost system resilience during these periods, thereby reducing the required capacity of LDS.

These composites confirm that, on average, depletion events in Widespread Innovation are characterised by more extreme high-pressure, low-temperature, and low-wind conditions. As shown in Chapter 4, depletion events in Widespread Innovation also tend to last for shorter periods within the overall duration of those in the Headwinds scenario. This indicates that the Widespread Innovation scenario only requires LDS when specific lower thresholds of temperature and wind speed are surpassed. Therefore, it can be concluded that Widespread Innovation is a more resilient scenario, less vulnerable to conditions that severely impact a lower-wind deployment scenario like Headwinds.

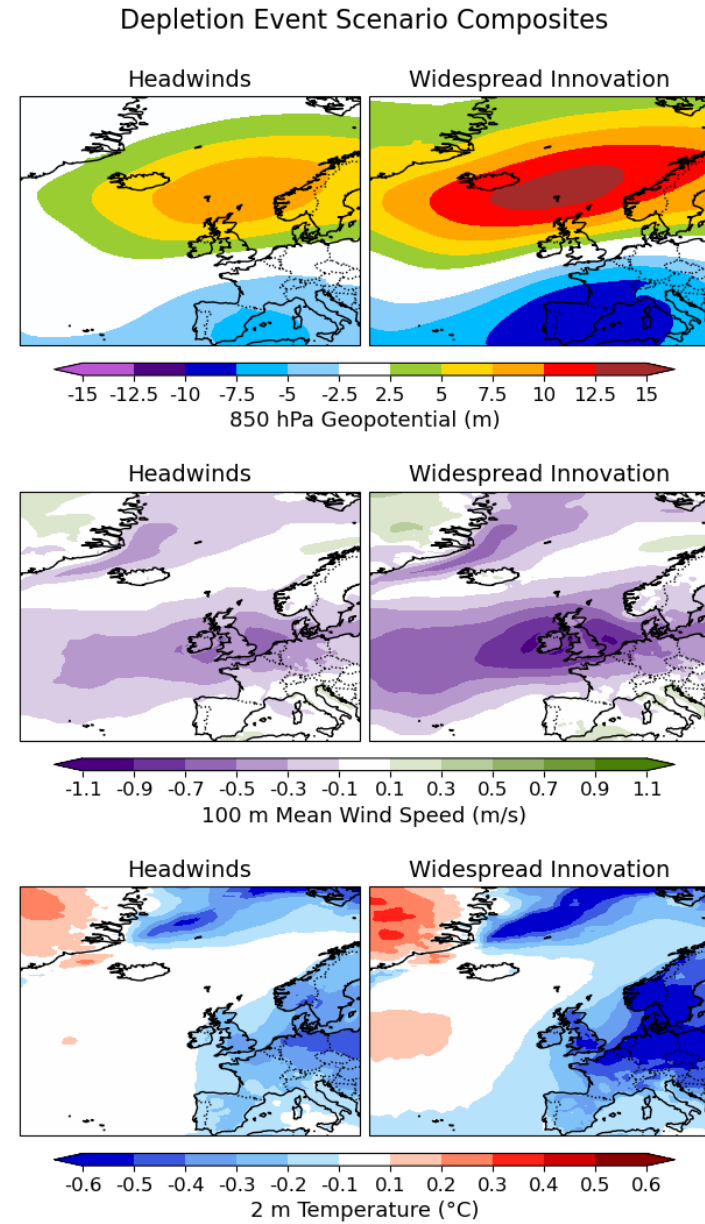


FIGURE 5.4: Composites of meteorological anomalies from climatology, taken for all months occurring during depletion events for the Headwinds (left column) and Widespread Innovation (right column) scenarios.

5.2.2 Changing Depletion Drivers

This section analyses the power variable anomalies to understand how changes in surface weather conditions translate into impacts on the energy systems in both scenarios.

In Fig. 4.2, shows a progressive reduction in storage needs for the 1959 event with increasing electrification and renewable deployment in energy systems. However, this reduction is less pronounced for the 1963 event. Consequently, the required storage capacity shifts from being primarily influenced by the 1959 event in the Headwinds and Balanced Pathway scenarios to being marginally influenced by the

1963 event in the Widespread Innovation scenario.

Both events occur within the same blocking period identified by Namias (1964), dominated by a 'High Scandinavia-Iceland' regime, and take place around the same time of year (October-March). This similarity suggests that the observed shift in storage requirements is driven by factors beyond synoptic conditions alone.

Both events occur within the same blocking period identified by Namias (1964), are dominated by a 'High Scandinavia-Iceland' regime, and take place around the same time of year (October-March). This similarity suggests that the observed shift in storage requirements is driven by factors other than synoptic conditions alone.

Fig. 5.5 presents the anomaly from climatology time series for supply, demand, and supply-net-demand for the two scenarios, covering both the 1959 and 1963 depletion events. The red highlights show the contribution of high demand to the supply-net-demand, indicating the impact of demand on the need for LDS.

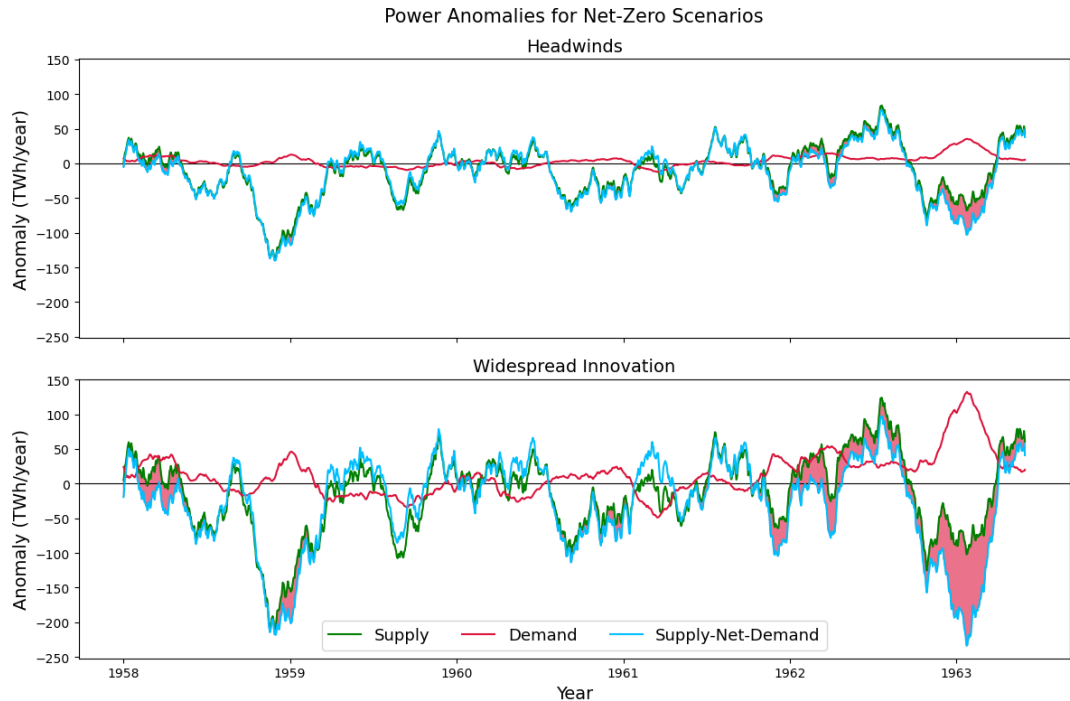


FIGURE 5.5: Supply, demand, and supply-net-demand power anomalies for the Headwinds and Widespread Innovation scenarios from 1959 to 1963. The shaded region highlights the contribution of demand to supply-net-demand anomalies, illustrating how increasing electrification causes higher demand for heating, making temperature a more significant driver of storage depletion.

In the Headwinds scenario, the demand anomaly during the 1959 event is only marginal, while the 1963 event shows a more significant anomaly. Across the board, the supply-net-demand anomaly is primarily driven by supply (i.e., wind). In the Widespread Innovation scenario, significant electrification leads to a substantial increase in demand anomalies. This is particularly evident in the 1963 event, where both demand and supply anomalies contribute similarly to the supply-net-demand anomaly.

For the same drop in temperature, the impact on demand is much more significant in the Widespread Innovation scenario. Consequently, both demand and wind are critical drivers of storage depletion in Widespread Innovation, whereas wind remains the predominant driver in Headwinds. These findings stress that the change in drivers is not due to a shift in weather patterns but rather a result of changes within the energy system itself.

This aligns with the findings of Bloomfield et al. (2020b), which noted that the deployment of wind power has already shifted the energy system from being primarily demand (temperature)-oriented to being sensitive to both temperature and wind. The present study suggests that future energy systems could revert back to being more temperature-sensitive, depending on the levels of wind power installed. This reiterates the previous discussion on the importance of maintaining adequate supply levels to support the decarbonisation of the heating sector.

5.3 Drivers Across the Historical Period

In this section, the anomaly fields of depletion events throughout the historical period are analysed to further distinguish the meteorological conditions driving the need for LDS.

K-means clustering is performed on the composite anomalies for each depletion event, focusing on geopotential, wind speed, and temperature. The four resulting cluster centers are shown in Fig. 5.6, while the corresponding meridional and zonal wind cluster centers are shown in Fig. D.1 in Appendix C.

These clusters are assigned to one or more weather regimes, identified through comparison with those illustrated in Lee et al. (2020).

- **Cluster 1 - NAO+:** Cluster 1 is characterised by a high-pressure anomaly extending from the Azores across to eastern Europe, with a trough over Greenland-Iceland, indicative of a NAO+ regime. This creates low pressure over Northern UK and higher pressure over Southern UK, resulting in an anomalous south-westerly wind and higher-than-normal wind speeds. Consequently, tropical maritime air masses lead to warmer, milder weather, as reflected in the above-normal temperatures.
- **Cluster 2 - NAO-:** Cluster 2 features a high-pressure anomaly north of Iceland and a trough centred over the Bay of Biscay, extending across southwestern Europe. This resembles an 'Icelandic high, trough over Central Europe' (HNZ), but with a less pronounced trough. The resulting lower pressure over the UK generates easterly winds with a moderate northerly component, leading to lower wind speeds and the influx of cold polar continental air masses. This brings cold weather and potential snow, indicated by the below-normal temperature anomalies over the UK.
- **Cluster 3 - Zonal ridge across Central Europe (BM):** Cluster 3 is marked by a ridge centred west of the British Isles, extending to Scandinavia and eastern Europe. This leads to an anomalous south-easterly wind over the UK, with higher-than-normal wind speeds in Northern UK and normal speeds in Southern UK. This pattern likely brings divided weather: calm, cooler conditions in the south from polar maritime or tropical maritime air masses,

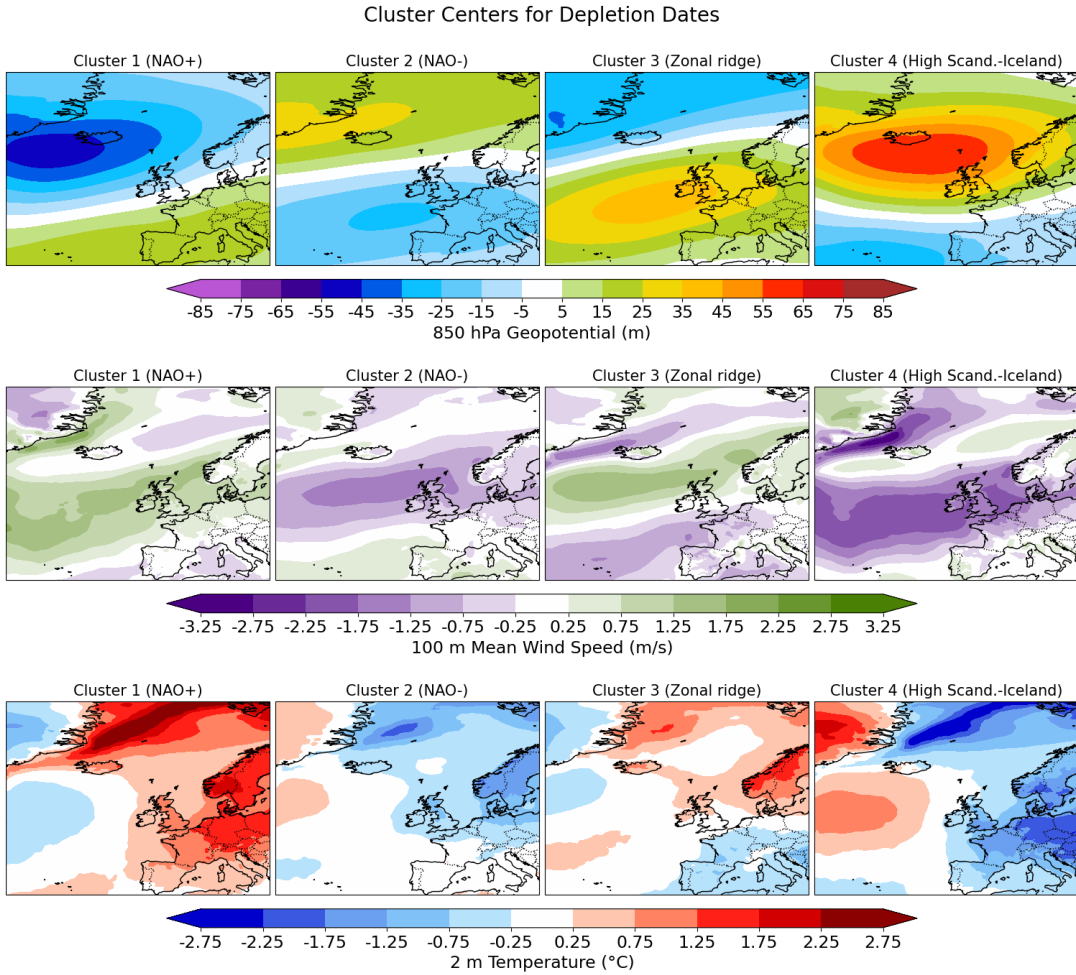


FIGURE 5.6: Cluster centers from k-means clustering of depletion event composites for Headwinds. Each center represents the average meteorological conditions of 850 hPa geopotential height, 100 m wind speed, and 2 m temperature during storage depletion.

and milder, windier conditions in Scotland from a warmer polar continental air mass.

- **Cluster 4 - High Scandinavia-Iceland, trough over Central Europe (HNFZ):** Cluster 4 is characterised by a pronounced high-pressure ridge between Iceland and Scandinavia, extending to central Europe. This results in an anomalous north-easterly wind over the UK, particularly strong in its easterly component, with overall lower wind speeds. This pattern likely brings cold polar continental air masses, leading to significantly colder conditions with potential snow, as indicated by the below-normal temperature anomalies. This cluster broadly resembles Scandinavian blocking-like conditions.

Drawing comparisons between the clusters provides insights into their anticipated impact on the UK energy system. Clusters 2 and 4, representing Greenland-Iceland blocking systems, are characterised by below-normal wind speeds and temperatures, likely resulting in simultaneous low supply and high demand. The deployment of LDS would be particularly pertinent for Cluster 4, as its pan-European effects would hinder the UK's ability to leverage interconnections

with nearby countries to counteract energy deficits.

Conversely, Clusters 1 and 3 are associated with normal to above-normal wind speeds and temperatures, suggesting they would not result in extreme low supply or high demand. This discrepancy indicates that the depletion event composites, derived from monthly mean data, do not adequately capture the meteorological conditions driving depletion on shorter timescales. Instead, these clusters likely represent conditions that recharge the store within overall periods of depletion.

Clusters 2 and 4 are further distinguished from Clusters 1 and 3 by their anomalous north-easterly wind component. The zonal component of Cluster 4, being over 2 s^{-1} stronger over the English Channel than that of the other clusters and having a significantly larger spatial extent, is its most distinguishing feature.

5.3.1 Consensus with the Literature

The identified meteorological conditions and their expected impacts on energy systems align well with current literature, particularly the study by Brayshaw et al. (2012), which also utilises the GWL classification.

Brayshaw et al. (2012) explicitly identified the Cluster 2 and Cluster 4 Iceland/Greenland blocking regimes as being colder and windier, thereby more susceptible to extreme demand. In the present study, this is found to be especially true for Cluster 4.

The study also noted that a 'High over the British Isles' regime would be unlikely to produce extreme peak demands on multi-annual timescales due to their association with low mean winds but more moderate temperatures. Cluster 3 in this study aligns with this regime, exhibiting above-normal wind speeds and temperatures, and is therefore less likely to have comparable impacts to Cluster 2 or Cluster 4.

A study on Dunkelflauten by Mockert et al. (2023) found that NAO- regimes are associated with the coldest weather in Germany. However, this study found that the High Scandinavian-Iceland blocking brings colder weather to both Germany and the UK.

Furthermore, Brayshaw et al. (2012) identified extended north-south troughs over western Europe as significant contributors to peak demand. While this study's clustering did not reveal such a trough regime, an extended trough was identified in Fig. 5.2, associated with low temperatures and wind speeds across the UK. The shorter durations of troughs compared to blocking ridge regimes may explain their lesser dominance in the post-compositing analysis, but they could still cause brief, significant storage discharges.

Additionally, Van Der Most et al. (2022) stated that extreme high shortfall events are driven by rare circulation types and small-scale features. As mentioned, clustering composites may average out expected features, and using only four clusters could prevent rare circulation types from being distinctly identified. These features may not be captured when considering 75 % variance over a large region like the NAE.

The limitations of this study's data resolution are further highlighted by a case study by Brayshaw et al. (2012), which identified a particularly cold 10-day spell in January 2010, consistent with various NAO-, Scandinavian blocking, and Atlantic ridge-aligned GWL regimes. This study's clustering analysis grouped the 2010 depletion event, occurring over the same period, into an NAO- regime. While this is

not necessarily inconsistent, it reinforces that daily-resolution data, on a case-by-case basis of depletion event, could provide better insights into the transient nature of blocking events relevant to LDS.

5.3.2 Clusters within a Historical Context

Considering these clustered depletion events within the context of the historical period provides valuable insights into the multi-annual impacts of these meteorological drivers on energy systems. The type of cluster associated with each depletion event is indicated in Fig. 5.7.

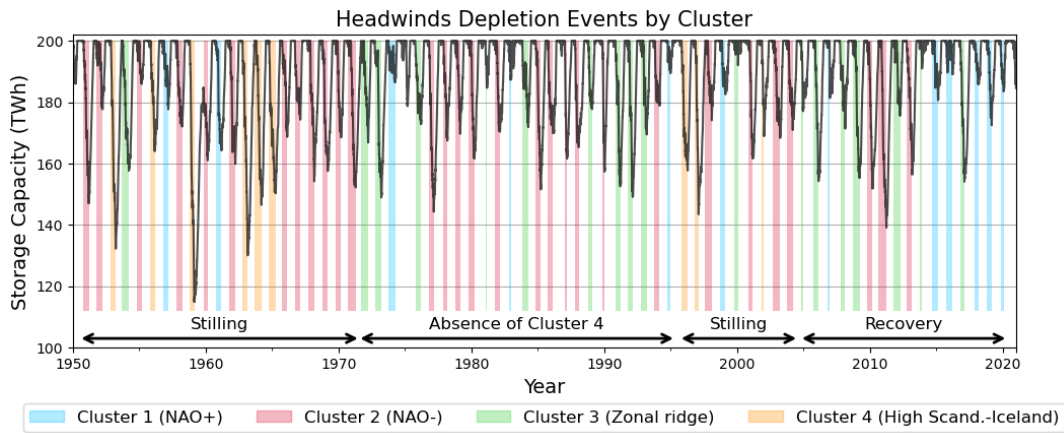


FIGURE 5.7: The Headwinds scenario storage from 1950-2022, with clusters corresponding to each identified depletion event indicated by colour.

NAO+ Cluster 1 events are the least frequent and most sporadic, accounting for just $\sim 17\%$ of all events. However, after 2010, Cluster 1 becomes the most frequent cluster, indicating a shift towards above-normal wind conditions. Clusters 2 and 3 occur more frequently, accounting for 44 % and 26 % of events respectively, while Cluster 4 is much less frequent, accounting for only 13 %.

Cluster 2 and Cluster 4 events often occur in multi-year successions throughout the 1950s to early 1970s. These lower-than-normal wind speeds characteristic of both clusters align with the period of wind stilling noted by Zhou et al. (2022). Notably, Cluster 2 occurs for six consecutive years in the late 1960s, representing the longest consecutive occurrence of any cluster type. The frequency of these clusters decreases after the 1980s, with an approximate 30-year period in which Cluster 4 events are absent. The mix of different clusters during this period aligns with Zhou et al. (2022), which found that this period corresponds to one which fluctuates in and out of wind stilling.

Cluster 3 occurs more frequently from 2005-2010, which is also found to be a period of above-average wind speeds in the 1980s and 1990s.

These findings, consistent with the literature, suggest that decadal wind speed variations significantly influence LDS depletion events.

5.3.3 Consensus with the Literature

These findings are cross referenced with the literature discussed in Section 2.4.1, in particular. Notably, Cluster 2 is found to be particularly persistent during the 1960s–1980s, aligning with The Royal Society’s findings that NAO+ events were less frequent during this period compared to 1980–2018.

Zhou et al. (2022) indicated that there was wind stilling over a period including the 1950s–1960s, which aligns with the increased frequency of Cluster 2 and cluster 4 events. The study found that there was a period of lesser stilling from 1970s–1990s, which aligns with absence for the post part of cluster 4 events, as well as the greater frequency of cluster 3 events relative to the 1950s and 1960s. The study then found that the wind stilling trend most decreased, and event reversed from the 1990s–2010s, with the dominance of cluster 3 and cluster 1 events during this period.

5.3.4 Clusters & Storage Capacity

To assess the distinct impact of each cluster on the need for LDS, the distribution of required storage for the clustered events is shown in Fig. 5.9.

Mann-Whitney U tests reveal no significant difference in the durations of the clusters. This is surprising, given that Mockert et al. (2023) found that Dunkelflauten tend to occur when a weather regime is well established and persists longer than usual. Therefore, one might expect the low-wind Cluster 4 to be associated with longer durations.

However, examining the correlation between the duration and magnitude of depletion events provides additional insight. A scatter plot analysis reveals a weak but significant ($p < .05$) Pearson correlation coefficient (0.31) between these variables. This suggests shared characteristics between the regimes beyond their geopotential anomalies.

Furthermore, Mann-Whitney U tests indicate that the distribution of required storage capacity for the clustered events differs significantly ($p < .05$) between all clusters, except between Cluster 2 and Cluster 3. Cluster 4, the Scandinavian blocking-like regime, while the least frequent, has the highest mean storage requirement of approximately 55 TWh. This suggests that if wind stilling is anticipated in future climates, storage capacity planning should consider the needs indicated by Cluster 4. Planning to a lesser capacity, such as that of the more frequent NAO- Cluster 2, may be more feasible if wind stilling is not expected, although it still carries some risk. Given the uncertainty surrounding the factors driving historic wind stilling and the debated evidence regarding its occurrence in future climates, a conservative approach that assumes wind stilling is likely would be prudent.

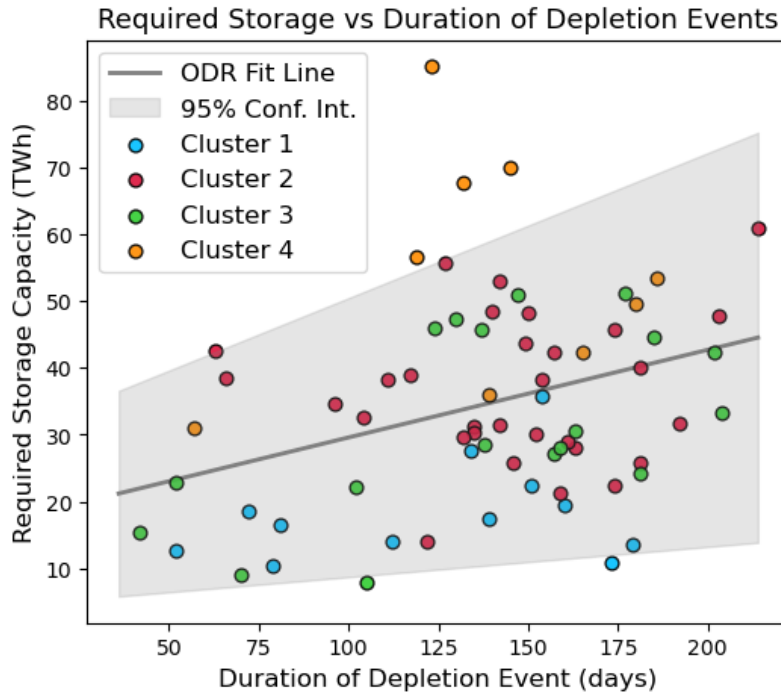


FIGURE 5.8: Duration of depletion events for the Headwinds scenario and the corresponding required storage capacity, categorised by cluster type. A linear orthogonal distance regression is applied to the data, with a 95 % confidence interval indicated by the shaded area.

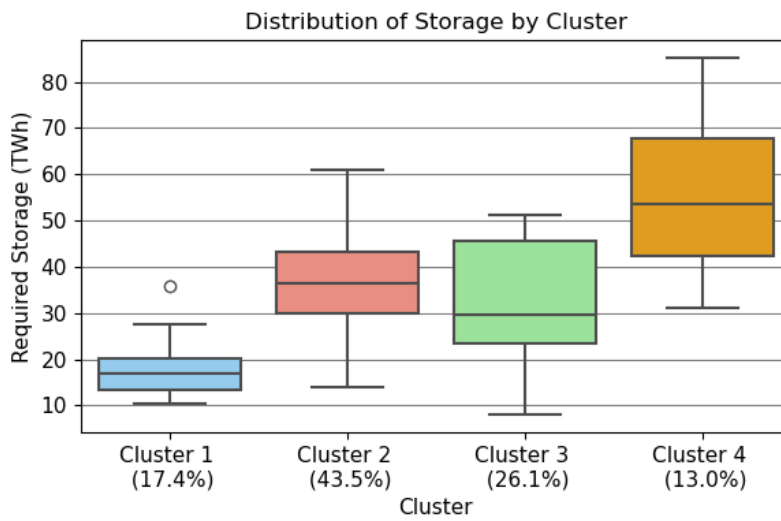


FIGURE 5.9: Distribution of required storage capacity by cluster, with percentages indicating the proportion of events in each cluster.

Chapter 6

Conclusions & Discussion

6.1 Conclusions

Achieving Net-Zero carbon emissions necessitates a transformative shift in the UK's energy landscape. This study investigates the need for Long-Duration Storage (LDS) and quantifies the capacity required to address energy deficits under various Net-Zero scenarios, each differing in technological and societal changes.

An underground hydrogen storage model and a 72-year ERA5-derived power dataset are used to quantify storage capacity and its associated uncertainties. The synoptic-scale meteorological conditions that drive storage depletion events are identified, with a detailed examination of the conditions causing the most prolonged and storage-intensive events.

Ultimately, the findings aim to inform more effective planning and investment in the deployment of LDS, thereby enabling a higher renewables, higher electrification, and low-carbon future for the UK. The following sections address the research questions posed in Chapter 1.

1. How much storage capacity will the UK require to meet energy deficits by 2050?

- (a) Does the required storage capacity vary depending on what pathway the UK takes to achieve Net-Zero?

By implementing three Net-Zero energy systems, constructed from the CCC's report, it is found that the answers to these two questions are intrinsically linked. Initial estimates of storage capacity are 88 TWh for Headwinds, 79 TWh for Balanced Pathway, and 49 TWh for Widespread Innovation.

When accounting for the uncertainty due to the finite data series and projected changes in storage conversion efficiencies, these estimates increase to 123 TWh, 85 TWh, and 49 TWh for the respective scenarios.

These findings suggest that a 2050 UK energy system characterised by high levels of renewable energy deployment, extensive electrification of heating, partial hydrogen adoption, and strong societal commitment to Net-Zero, requires the least LDS. Counterintuitively, a future with less technological advancement, limited offshore renewables deployment, and greater reliance on CCS technologies requires up to 2.5 times more LDS capacity. A balanced scenario, combining both electrification and hydrogen for heating, has storage requirements between these extremes.

The vulnerability of the Headwinds energy system is particularly evident, as it not only requires the highest initial LDS estimate but also the highest contingency to ensure a reliable power supply. This is conceptualised as 'resilience'—the ability to withstand prolonged periods of high demand and low supply. This finding raises concerns that highly advanced scenarios akin to Widespread Innovation, but without adequate supply levels, would struggle to meet the deficits posed by the electrification of demand.

Overall, while the analysis of these three scenarios provides valuable insights, they primarily explore a two-dimensional plane defined by the electrification of demand and the deployment of offshore wind power. Future research should consider additional dimensions, such as hydrogen adoption, to provide a more nuanced understanding of the need for LDS in a Net-Zero energy landscape.

(b) How do these estimates compare to those found in existing literature?

The initial estimates of storage capacity in this study (49 TWh to 88 TWh) run lower than those found in LDS-focused literature, such as Domeisen (2019). However, they are higher than estimates from comprehensive system-wide studies like the CCC (2020a) report, which explicitly include interconnection and nuclear power. These higher estimates in the present study can be partially attributed to the inclusion of an extended historical period, encompassing the wind-stilling, consecutive blocking events of the 1950s–1960s.

The Royal Society's report, which suggests a capacity of 123 TWh, inclusive of an uncertainty for weather and climate variability, aligns closely with this study's suggested 123 TWh for the Headwinds scenario, which also includes an additional uncertainty for conversion efficiencies. Differences in modelling assumptions, particularly regarding the inclusion of a baseload and the electrification of demand, are suggested to obscure the true disparity between the two studies.

Overall, despite the simplicity of the storage and Net-Zero scenario modelling employed in this study, the findings align well with the existing literature.

2. What meteorological drivers govern the storage capacity required by the UK?

A case study on the most severe depletion event revealed it coincided with a high-pressure ridge forming over Scandinavia, enabled by SST and snow-precipitation-temperature feedbacks. Following an SSW event, an NAO-tripole pressure regime reinforced cold, low-wind conditions over the UK.

K-means clustering of depletion events across the historical period identified four types of regimes. Two clusters, indicative of lower-than-normal wind and temperatures, correspond to blocking systems over Britain and Scandinavia-Iceland. The latter is associated with the highest storage requirement of all identified clusters. Although less frequent, these conditions are notable during historical periods of wind stilling, indicating the need to consider future stilling in LDS planning. This cluster also tends to have pan-European impacts, increasing the need for LDS due to reduced interconnection opportunities.

(a) Do these meteorological drivers vary depending on the pathway the UK take to achieve Net-Zero?

Composite analysis of meteorological variable field anomalies shows that more advanced scenarios are broadly driven by the same synoptic blocking systems as less advanced scenarios. However, due to a higher level of overall wind supply, the high-wind scenarios only require LDS when temperatures and wind speeds drop below certain thresholds.

Analysis of UK power anomalies reveals that in scenarios characterised by lower renewables deployment and lower electrification of demand, wind is the primary meteorological driver of depletion. In contrast, scenarios with higher levels of renewables and significant electrification of heating demand see both low wind and low temperatures as critical drivers of depletion.

Overall, while high-wind, high-electrification scenarios exhibit an additional temperature-driven component, their greater resilience due to increased wind power makes them less vulnerable to extreme conditions.

6.2 Discussion

What are the major limitations or sources of uncertainty of this study?

System Interactions

The simplicity of the underground storage model and its limited interactions with other components of the energy system and market are a fundamental limitation of this study. For instance, the dynamic modelling of nuclear energy does not account for nuclear co-generation where their operations are intrinsically linked. A nuclear operator might, for example, increase generation output during times of energy surplus to charge the LDS system in anticipation of a later deficit. The current model also does not consider instances where surplus renewable or nuclear energy may be sold to neighbouring countries via interconnectors when it is profitable to do so, instead of charging the store. These factors combined could alter the estimated storage capacity requirements.

Furthermore, given the significant influence of economic markets on the energy grid and, in turn, LDS, it is crucial to incorporate market dynamics in LDS modelling. Ignoring these factors could lead to inaccurate estimates of storage capacity, as market-driven decisions would affect the timing and amount of energy stored or released, as well as the feasibility of deploying LDS systems.

Advanced methods like agent-based modelling and econometric models could offer a more realistic representation of LDS dynamics. However, if fully complex market modelling is not feasible, some level of economic consideration can still be integrated. Dowling et al. (2020) demonstrated this by optimising storage capacities and dispatch to minimise system costs, which can enhance the robustness of storage capacity estimates.

Generalisability

The methodology of applying a power reanalysis dataset, representative of the 2017-2022 energy system, and adapting it to model a 2050 system introduces inherent limitations. This approach particularly affects the generalisability of the demand and supply modelling to highly electrified and high-wind Net-Zero scenarios beyond the scope of this study.

In terms of supply, the assumption that RE supply variability scales with the square of installed capacity may not hold if there are substantial changes in RE deployment patterns or improvements in grid management. For example, advanced demand-side response measures could encourage higher electricity consumption during periods of high renewable generation, potentially reducing overall supply variability. The CCC does not provide specific figures on intra-annual supply variability, making this scaling assumption a necessary proxy.

Additionally, the scaling assumes that the distribution of wind and solar farms remains unchanged by 2050. However, a high-wind scenario could lead to significant changes in the location of offshore wind farms, potentially altering national aggregate capacity factors. Furthermore, extensive wind and solar deployment might result in increased curtailment during periods of excess generation, causing capacity factors to stabilise rather than increase proportionally with installed capacity, as currently assumed.

In terms of demand, the modelling depends on manual fine-tuning based on estimates from various external sources, raising concerns about the accuracy and reliability of the approach. The demand modelling could be improved by using historical gas demand data over a longer period, such as one year, to model the electrification of demand more accurately.

Overall, the main limitation of this study lies in its modelling of supply and demand. This affects the generalisability of this study's methodology to scenarios with higher levels of electrification and wind deployment than those in Widespread Innovation.

Temporal Resolution

While the LDS depletion events discussed in Chapter 5 are prolonged and occur over 1-4 month periods, using monthly-mean data tends to average out brief but significant weather conditions within this time. Consequently, shorter periods that cause sudden storage discharge are not represented in the monthly-mean field composite. This averaging can lead to misleading conclusions, such as the identification of Clusters 1 and 3, which inaccurately attribute high wind and low temperatures as primary causes of depletion. Utilising daily-mean data, though computationally expensive, would provide deeper insights into the frequency and dominance of the various weather regimes within each event.

The impact of using monthly-mean data is also evident when selecting the optimal number of clusters from the elbow point in Fig. 3.4. While an 'elbow' at 4 clusters is a reasonable choice, the absence of a well-defined elbow suggests that the data either lacks strong natural groupings as they are naturally overlapping or spread out in the feature space. To address this, a weighted covariance matrix could be applied over the NAE domain prior to PCA. Emphasising the UK region more heavily could lead to more meaningful results in the context of examining UK energy systems.

What research opportunities could future studies address?

Aside from the recommendations made, there are several avenues for future research, particularly in increasing modelling confidence.

Net-Zero Scenario Modelling

Focusing on Net-Zero scenarios with realistic assumptions can enhance the accuracy and relevance of LDS modelling efforts. The most recent National Grid (2024) report narrows its focus to fuel switching to hydrogen and electrification while maintaining both demand-side and supply-side flexibility. Although the Committee on Climate Change's Sixth Carbon Budget provided the foundation for the scenarios in this study, its Balanced Pathway scenario, which included a mix of hydrogen and electrified heating, is insufficient to explore the full extent of hydrogen fuel switching.

Therefore, future research should model LDS needs using insights from the 2024 FES report regarding fuel switching. Such research could determine whether a higher or lower need for hydrogen storage is required, depending on the degree of hydrogen fuel switching alongside electrification.

Furthermore, despite adopting the CCC's own Net-Zero pathways, their corresponding LDS estimates differ substantially from this study's, more than any other literature examined. It is unclear from their documentation how exactly these LDS estimates were modelled. To investigate this further, an inverse experiment could be performed, simulating a UK energy system with their recommended level of capacity and working backwards to determine the energy deficits this would entail.

Supply and Demand Modelling

Future research opportunities in supply and demand modelling could focus on advanced weather and climate modelling or enhanced energy network modelling.

Firstly, the current study is inherently limited by the finite historical record of homogeneous weather data. Future research could benefit from using ensembles from global climate models, such as EC-Earth and HadGEM2, to obtain multi-century records of simulated weather data for present-day conditions. This approach could offer a superior alternative to the Monte Carlo resampling method and provide deeper insights into the severity, return period, and associated weather regimes of extreme events. Climate-change models could also enable a more quantitative approach to understanding how climate-change-induced weather patterns may impact a highly renewable electricity system, facilitating robust planning for an energy system suitable for 2050 while minimising the need for significant overhauls in the future.

Additionally, while this study extensively analysed the UK power system, the framework can be adapted for future analyses in other countries. It is possible to construct a multi-country interconnection system, where each country has its own LDS and dynamic nuclear baseload. This approach could assume that the UK's Net-Zero scenarios are applicable to other countries with similar populations and economic structures, such as France, Spain, and Germany. Alternatively, each country's Net-Zero framework could be considered on an individual basis. Another promising area for future research is modelling a UK-Europe energy system as a whole, without considering each country separately. Examining the meteorological drivers across such interconnected systems could identify regions with poorly correlated LDS meteorological drivers, optimising resource sharing and reducing the collective need for LDS.

Appendix A

Literature Review

TABLE A.1: Overview of Net-Zero scenarios from three reports by the Committee on Climate Change (2020c); National Grid (2023b), and Barrett (2021).

Organisation	Scenario	Shorthand	Description
NG	Falling Short	NG-FS	Slowest credible pathway to Net-Zero, failing to meet the 2050 target. Minimal change to consumer behaviour. Heavy reliance on natural gas, particularly for domestic heating. Some EV take-up, as well as low hydrogen adoption.
	System Transformation	NG-ST	More supply-side flexibility, with consumers less inclined to change behaviours than in CCC-CT and with lower energy efficiency levels. Features electrified heating. Highest proportion of hydrogen across the NG scenarios.
	Consumer Transformation	NG-CT	Consumers are willing to change behaviour resulting in demand-side flexibility. Features high energy efficiencies. Home heating, transport, and industry are largely electrified. Some hydrogen use in electricity generation.
	Leading the Way	NG-LTW	Fastest credible pathway to Net-Zero. Features significant consumer lifestyle change. Combination of hydrogen and electricity used in industry and home heating.
CCC	Headwinds	CCC-HW	No widespread behavioural shifts or innovations that facilitate the emergence of cost-reduction technologies. Reliant on hydrogen and CCS technologies to achieve Net-Zero.
	Balanced Pathway	CCC-BP	Informed by the four other pathways. Makes moderate assumptions on consumer change and innovations, leaves leeway for a range of ways of reaching Net-Zero.
	Widespread Engagement	CCC-WE	High levels of consumer behavioural changes, reducing demand for carbon-intensive activities. Cost reduction assumptions are similar to CCC-HW.

TABLE A.1: (continued)

Organisation	Scenario	Shorthand	Description
Widespread Innovation	Widespread Innovation	CCC-WI	Assumes success in cost-reduction technologies which enables widespread electrification and greater levels of energy efficiency. Consumer changes are similar to CCC-HW.
	Tailwinds	CCC-TW	Successes in both societal mitigation and innovative methods that goes further beyond CCC-BP in reaching Net-Zero prior to 2050.
CREDS	Ignore demand	CREDS-I	Ignore: Considers achieving energy demand reductions, based on established UK policies in 2018, rather than planned ambitions. Significantly fails to approach Net-Zero.
	Steer demand	CREDS-ST	Maintains energy service demands as in CREDS-I, but is constrained to reach Net-Zero. Relies on improved energy efficiency, supply-side flexibility, and CDR technologies. No consumer behavioural changes.
	Shift demand	CREDS-SH	Significant shift in the attention to demand-side flexibility with an ambitious programme of interventions across the whole economy. Makes use of existing technologies and current social framings.
	Transform demand	CREDS-T	Reflects transformative change in consumer behaviour, technological developments, and institutions work in tandem to deliver energy reductions.

Appendix B

Data & Methods

B.1 Scenario Selection

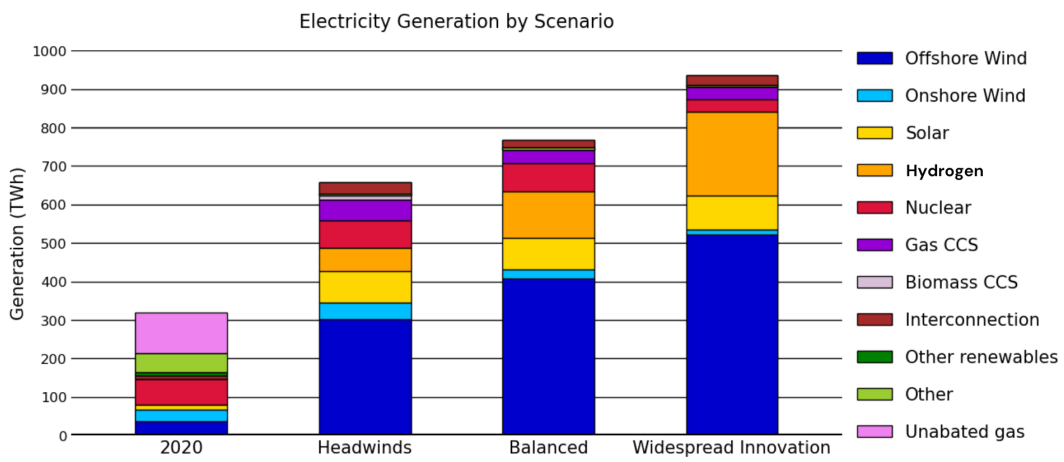


FIGURE B.1: Electricity generation in 2050 reported by the Committee on Climate Change for the three selected Net-Zero scenarios, as well as the Balanced Pathway in 2022.

B.2 Quantifying Storage Capacity

A methodology was constructed to define depletion peaks and events, ensuring consistency and generalisation across the three scenarios. Local minima within a 170-day window were identified to capture one significant peak per winter-spring period. This method is appropriate for Headwinds and Balanced Pathway, which typically have a single major event during this time. However, in Widespread Innovation, which often has a main peak along with secondary peaks, these secondary peaks are treated as part of the recovery period. Distinguishing these secondary peaks without compromising robustness remains a challenge.

Depletion events are defined to start at the last instance before a peak, where storage remains below 3 TWh for at least 20 consecutive days. These values were chosen based on visual analysis for optimal accuracy. If storage does not recover above this threshold between peaks, the event starts from the last local minimum following the prior peak. This method ensures accurate distinction of consecutive depletion events, such as the 1959-1960 events in Headwinds.

B.3 Demand

The CCC supplies only mean annual demand levels for 2050. However, additional figures for peak demand and intraannual variability are required to adjust the variability and seasonal cycle of demand. These additional figures are derived as follows:

- **Peak Demand:** Derived from National Grid (2023b) for scenarios analogous to this study's scenarios (Headwinds – Falling Short, Balanced Pathway – Consumer Transformation, Widespread Innovation – System Transformation), discussed in Chapter 2.
- **Intraannual Variability:** Derived from Ehsan and Preece (2022), which constructed scenarios based on the National Grid (2023b) analogous scenarios.

The analogous scenarios present slightly higher and lower mean annual demands than Balanced Pathway and Widespread Innovation, respectively. Therefore, these peak demand and intra-annual variability figures serve as upper and lower bounds for the Balanced Pathway and Widespread Innovation scenarios. Due to the iterative nature of scaling demand, the actual peak demand and intra-annual variability values attained do not exactly match these figures but lie towards the lower and upper ends of their respective ranges. Table 3.1 shows these upper and lower range values, alongside the value attained in brackets.

The nature of Net-Zero modelling in this study, which relies on external literature, faces an inherent limitation in balancing transparency and the availability of desired figures.

Appendix C

Quantifying Storage

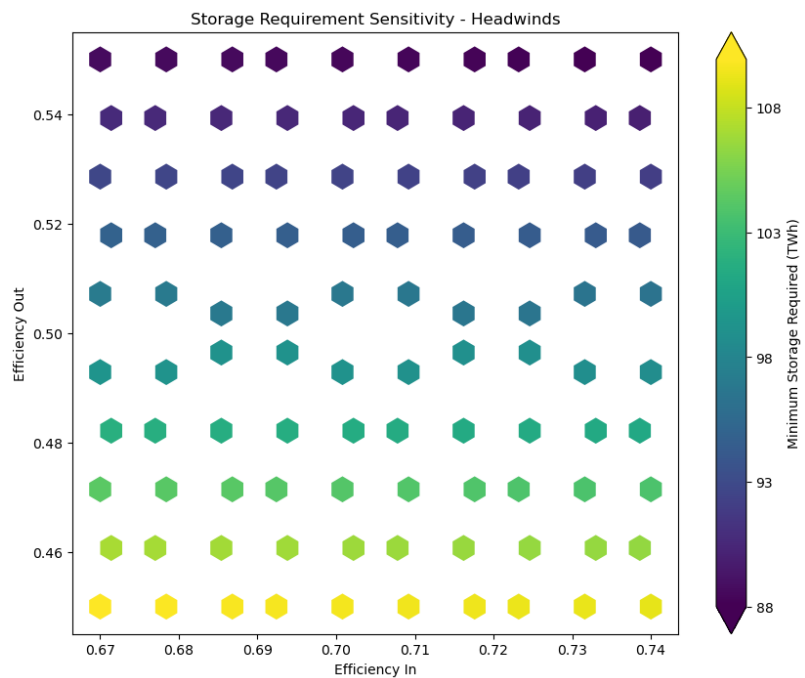


FIGURE C.1: Required storage capacity in Headwinds for various input and output LDS conversion efficiencies.

Appendix D

Identifying Meteorological Drivers

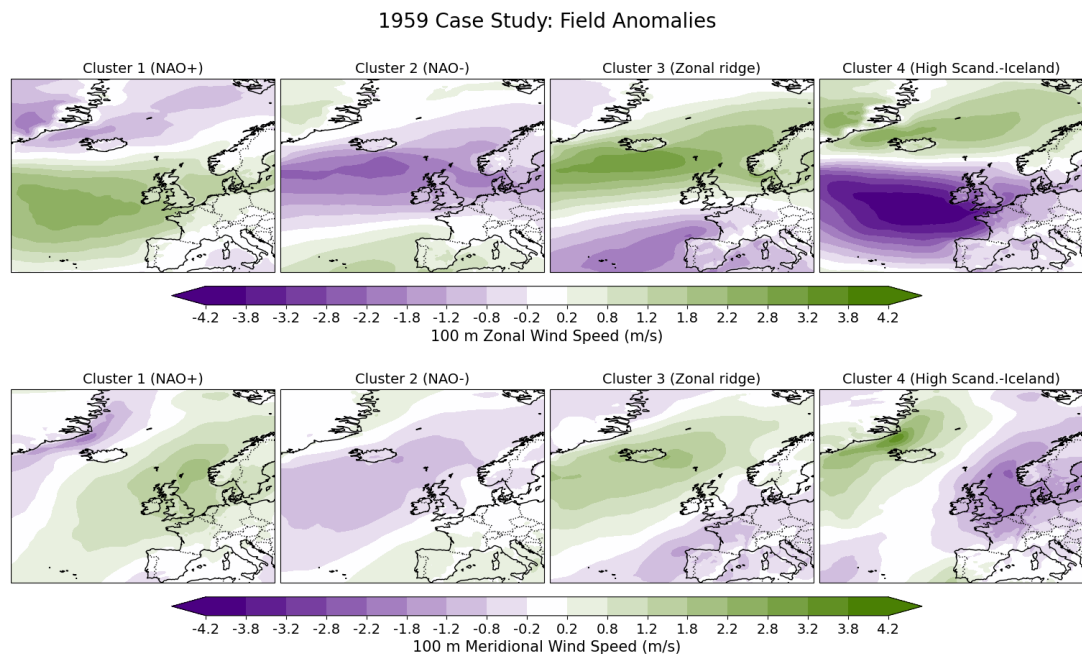


FIGURE D.1: Cluster centers for the zonal (top) and meridional (bottom) wind speeds from k-means clustering of depletion event composites for Headwinds.

References

- Arup, 2023: Assessing the regional demand for geological hydrogen storage: Building a strategic case for investment in the east coast cluster. Tech. rep. <https://www.arup.com/globalassets/downloads/insights/a/assessing-the-regional-demand-for-geological-hydrogen-storage.pdf>.
- Barrett, J., 2021: The role of energy demand reduction in achieving net-zero in the UK. Tech. rep., The Centre for Research into Energy Demand Solutions, 1-86 pp. <https://www.creds.ac.uk/wp-content/uploads/CREDS-Role-of-energy-demand-report-2021.pdf>.
- Bloomfield, H., D. Brayshaw, and A. Charlton-Perez, 2020a: ERA5 derived time series of European country-aggregate electricity demand, wind power generation and solar power generation. University of Reading, Accessed 28 July 2024, <https://doi.org/10.17864/1947.273>.
- Bloomfield, H. C., D. J. Brayshaw, and A. J. Charlton-Perez, 2020b: Characterizing the winter meteorological drivers of the European electricity system using targeted circulation types. *Meteorological Applications*, **27** (1), 1–18, <https://doi.org/10.1002/met.1858>.
- Bloomfield, H. C., D. J. Brayshaw, M. Deakin, and D. Greenwood, 2022: Hourly historical and near-future weather and climate variables for energy system modelling. *Earth System Science Data*, **14** (6), 2749–2766, <https://doi.org/10.5194/essd-14-2749-2022>.
- Bloomfield, H. C., D. J. Brayshaw, L. C. Shaffrey, P. J. Coker, and H. E. Thornton, 2018: The changing sensitivity of power systems to meteorological drivers: a case study of Great Britain. *Environmental Research Letters*, **13** (5), 1–11, <https://doi.org/10.1088/1748-9326/aabff9>.
- Bolton, P., 2024: Gas and electricity prices under the Energy Price Guarantee and beyond. Research briefing, House of Commons Library, 1-6 pp. <https://researchbriefings.files.parliament.uk/documents/CBP-9714/CBP-9714.pdf>.
- Brayshaw, D. J., C. Dent, and S. Zachary, 2012: Wind generation's contribution to supporting peak electricity demand-meteorological insights. *Proceedings of the Institution of Mechanical Engineers, Part O: Journal of Risk and Reliability*, **226** (1), 44–50, <https://doi.org/10.1177/1748006X11417503>.
- Centre for Research into Energy Demand Solutions, 2022: Positive low energy futures. Accessed 5 August 2023, <https://low-energy.creds.ac.uk/the-report/>.
- Charlton-Perez, A., L. Ferranti, and R. W. Lee, 2018: The influence of the stratospheric state on North Atlantic weather regimes. *Q. J. R. Meteor. Soc.*, **144** (713), 1140–1151, <https://doi.org/10.1002/qj.3280>.

- Climate Watch, 2024: Net-zero tracker. Accessed 15 June 2024, <https://www.climatewatchdata.org/net-zero-tracker>.
- Committee on Climate Change, 2020a: Sixth carbon budget - charts and data in the report. Accessed 5 August 2024, <https://www.theccc.org.uk/publication/sixth-carbon-budget/>.
- Committee on Climate Change, 2020b: The sixth carbon budget: Methodology report. Tech. rep., 1-340 pp. <https://www.theccc.org.uk/wp-content/uploads/2020/12/The-Sixth-Carbon-Budget-Methodology-Report.pdf>.
- Committee on Climate Change, 2020c: The sixth carbon budget: The UK's path to net zero. Tech. rep., 1-448 pp. <https://www.theccc.org.uk/wp-content/uploads/2020/12/The-Sixth-Carbon-Budget-The-UKs-path-to-Net-Zero.pdf>.
- Committee on Climate Change, 2023: Delivering a low-carbon, reliable power system. Tech. rep., 10-110 pp. <https://www.theccc.org.uk/wp-content/uploads/2023/03/Delivering-a-reliable-decarbonised-power-system.pdf>.
- Department for Business, E., and I. Strategy, 2021: Impact assessment for the sixth carbon budget. Tech. Rep. BEIS012(F)-21-CG, 1-59 pp. https://www.legislation.gov.uk/ukia/2021/18/pdfs/ukia_20210018_en.pdf.
- Department for Business, Energy Industrial Strategy, 2023: Energy security bill factsheet: Multi-purpose interconnectors. Accessed 6 August 2024, <https://www.gov.uk/government/publications/energy-security-bill-factsheets/energy-security-bill-factsheet-multi-purpose-interconnectors>.
- Department for Energy Security and Net Zero, 2023: Hydrogen strategy delivery update. Tech. rep., 14 pp. <https://assets.publishing.service.gov.uk/media/65841578ed3c3400133bfcf7/hydrogen-strategy-update-to-market-december-2023.pdf>.
- Department for Energy Security and Net Zero, 2024: 2022 UK greenhouse gas emissions, final figures. Government report, 14 pp. <https://assets.publishing.service.gov.uk/media/65cd015863a23d0031c82e1e9/2022-final-greenhouse-gas-emissions-statistical-release.pdf>.
- Department for Energy Security and Net Zero and Department for Business, Energy and Industrial Strategy, 2019: Nuclear electricity in the UK. Government report, 66 pp. <https://www.gov.uk/government/publications/energy-trends-march-2019-special-feature-article-nuclear-electricity-in-the-uk>.
- Department for Energy Security and Net Zero and Department for Business, Energy and Industrial Strategy, 2021: Net zero strategy: Build back greener. Tech. rep., HM Government, UK. <https://www.gov.uk/government/publications/net-zero-strategy-build-back-greener>.
- Department for Energy Security and Net Zero and Department for Business, Energy and Industrial Strategy, 2022: Fugitive hydrogen emissions in a future hydrogen economy. Tech. rep., 1-52 pp. <https://assets.publishing.service.gov.uk/media/624ec79cd3bf7f600d4055d1/fugitive-hydrogen-emissions-future-hydrogen-economy.pdf>.
- Det Norske Veritas, 2022: Hydrogen forecast to 2050. Tech. rep. https://abn.com.br/wp-content/uploads/2022/06/DNV_Hydrogen_Report_2022_Highres_single1.pdf.

- Domeisen, D. I. V., 2019: Estimating the frequency of sudden stratospheric warming events from surface observations of the North Atlantic Oscillation. *J. Geophys. Res.: Atmospheres*, **124** (6), 3180–3194, <https://doi.org/10.1029/2018JD030077>.
- Dowling, J. A., K. Z. Rinaldi, T. H. Ruggles, S. J. Davis, M. Yuan, F. Tong, N. S. Lewis, and K. Caldeira, 2020: Role of long-duration energy storage in variable renewable electricity systems. *Joule*, **4** (9), 1907–1928, <https://doi.org/10.1016/j.joule.2020.07.007>.
- Eggimann, S., W. Usher, N. Eyre, and J. W. Hall, 2020: How weather affects energy demand variability in the transition towards sustainable heating. *Energy*, **195**, 116947, <https://doi.org/10.1016/j.energy.2020.116947>.
- Ehsan, A., and R. Preece, 2022: Quantifying the impacts of heat decarbonisation pathways on the future electricity and gas demand. *Energy*, **254**, 1–10, <https://doi.org/10.1016/j.energy.2022.124229>.
- Fankhauser, S., and Coauthors, 2022: The meaning of net zero and how to get it right. *Nature Climate Change*, **12** (1), 15–21, <https://doi.org/10.1038/s41558-021-01245-w>.
- Grams, C. M., R. Beerli, S. Pfenninger, I. Staffell, and H. Wernli, 2017: Balancing Europe's wind-power output through spatial deployment informed by weather regimes. *Nature Climate Change*, **7** (8), 557–562, <https://doi.org/10.1038/nclimate3338>.
- Grochowicz, A., K. van Greevenbroek, and H. C. Bloomfield, 2024: Using power system modelling outputs to identify weather-induced extreme events in highly renewable systems. *Environmental Research Letters*, **19** (5), 3–4, <https://dx.doi.org/10.1088/1748-9326/ad374a>.
- H2eart for Europe, 2024: The role of underground hydrogen storage in Europe. Tech. rep., 1–47 pp. https://h2eart.eu/wp-content/uploads/2024/01/H2eart-for-Europe_Report_Role-of-UHS-in-Europe.pdf.
- Hassan, Q., S. Algburi, A. Z. Sameen, H. M. Salman, and M. Jaszczur, 2023: A review of hybrid renewable energy systems: Solar and wind-powered solutions: Challenges, opportunities, and policy implications. *Results in Engineering*, 1–3, <https://doi.org/10.1016/j.rineng.2023.101621>.
- Hilbers, A. P., D. J. Brayshaw, and A. Gandy, 2020: Efficient quantification of the impact of demand and weather uncertainty in power system models. *IEEE Transactions on Power Systems*, **36** (3), 1771–1779, <https://doi.org/10.1109/TPWRS.2020.3031187>.
- Hydrogen UK, 2023: Hydrogen storage: Delivering on the UK's energy needs. Tech. rep., 1–6 pp. URL <https://hydrogen-uk.org/publication/hydrogen-storage-delivering-on-the-uks-energy-needs/>.
- Jenkins, J. D., and N. A. Sepulveda, 2021: Long-duration energy storage: A blueprint for research and innovation. *Joule*, **5** (9), 2241–2246, <https://doi.org/10.1016/j.joule.2021.08.002>.
- Joffe, D., S. Livermore, and M. Hemsley, 2018: Hydrogen in a low-carbon economy. Tech. rep., Committee on Climate Change. <https://www.theccc.org.uk/wp-content/uploads/2018/11/Hydrogen-in-a-low-carbon-economy.pdf>.

- Johnson, E., S. Betts-Davies, and J. Barrett, 2023: Comparative analysis of UK net-zero scenarios: The role of energy demand reduction. *Energy Policy*, **179**, 1–12, <https://doi.org/10.1016/j.enpol.2023.113620>.
- Karpechko, A. Y., A. Charlton-Perez, M. Balmaseda, N. Tyrrell, and F. Vitart, 2018: Predicting sudden stratospheric warming 2018 and its climate impacts with a multimodel ensemble. *J. Geophys. Res.: Atmospheres*, **45** (24), 13–538, <http://dx.doi.org/10.1029/2018GL081091>.
- Kimpton, S. K., C. Taylor, C. W. Thomson, N. Robertson, and C. West, 2023: Role of hydrogen storage for UK energy resilience for net zero. Conference paper. Accessed 6 August 2024, <https://doi.org/10.2118/215489-MS>.
- King, A. D., A. H. Butler, M. Jucker, N. O. Earl, and I. Rudeva, 2019: Observed relationships between sudden stratospheric warmings and European climate extremes. *J. Geophys. Res.: Atmospheres*, **124** (24), 13 943–13 961, <https://doi.org/10.1029/2019JD030480>.
- Koehler, E., E. Brown, and S. J.-P. Haneuse, 2009: On the assessment of Monte Carlo error in simulation-based statistical analyses. *The American Statistician*, **63** (2), 155–162, <https://doi.org/10.1198/tast.2009.0030>.
- Lee, J. C. K., R. W. Lee, S. J. Woolnough, and L. J. Boxall, 2020: The links between the Madden-Julian Oscillation and European weather regimes. *Theoretical and Applied Climatology*, **141** (1), 567–586, <https://doi.org/10.1007/s00704-020-03223-2>.
- Marcheggiani, A., J. Robson, P.-A. Monerie, T. J. Bracegirdle, and D. Smith, 2023: Decadal predictability of the North Atlantic eddy-driven jet in winter. *Geophysical Research Letters*, **50** (8), 1–9, <https://doi.org/10.1029/2022GL102071>.
- Martius, O., L. M. Polvani, and H. C. Davies, 2009: Blocking precursors to stratospheric sudden warming events. *Geophysical Research Letters*, **36** (14), 1–4, doi:<https://doi.org/10.1029/2009GL038776>, Accessed 28 July 2024, <https://doi.org/10.1029/2009GL038776>.
- Masson-Delmotte, V., and Coauthors, 2021: Climate change 2021: The physical science basis. *Contribution of working group I to the sixth assessment report of the Intergovernmental Panel on Climate Change*, **2** (1), 2391, <https://doi.org/10.1017/9781009157896>.
- Michelangeli, P.-A., R. Vautard, and B. Legras, 1995: Weather regimes: Recurrence and quasi stationarity. *J. Atmos. Sci.*, **52** (8), 1237–1256, [http://dx.doi.org/10.1175/1520-0469\(1995\)052<1237:WRRAQS>2.0.CO;2](http://dx.doi.org/10.1175/1520-0469(1995)052<1237:WRRAQS>2.0.CO;2).
- Minola, L., C. Azorin-Molina, and D. Chen, 2016: Homogenization and assessment of observed near-surface wind speed trends across Sweden, 1956–2013. *Journal of Climate*, **29** (20), 7397–7415, <https://doi.org/10.1175/JCLI-D-15-0636.1>.
- Mockert, F., C. M. Grams, T. Brown, and F. Neumann, 2023: Meteorological conditions during periods of low wind speed and insolation in Germany: The role of weather regimes. *Meteor. Appl.*, **30** (4), 1–11, <https://doi.org/10.1002/met.2141>.
- Mouli-Castillo, J., N. Heinemann, and K. Edlmann, 2021: Mapping geological hydrogen storage capacity and regional heating demands: An applied UK case study. *Applied Energy*, **283**, 1–10, <https://doi.org/10.1016/j.apenergy.2020.116348>.

- Mulvaney, D., J. Busby, and M. D. Bazilian, 2020: Pandemic disruptions in energy and the environment. *Elementa: Science of the Anthropocene*, **8** (1), 1–7, <https://doi.org/10.1525/elementa.052>.
- Muthén, L. K., and B. O. Muthén, 2002: How to use a Monte Carlo study to decide on sample size and determine power. *Structural equation modeling*, **9** (4), 599–620, https://doi.org/10.1207/S15328007SEM0904_8.
- Namias, J., 1964: Seasonal persistence and recurrence of European blocking during 1958–1960. *Tellus*, **16** (3), 394–407, <https://doi.org/10.1111/j.2153-3490.1964.tb00176.x>.
- National Grid, 2019: De-rating factor methodology for renewables participation in the capacity market. Accessed 31 August 2021, <https://www.emrdeliverybody.com/Capacity%20Markets%20Document%20Library/EMR%20DB%20Consultation%20response%20-%20De-rating%20Factor%20Methodology%20for%20Renewables%20Participation%20in%20the%20CM.pdf>.
- National Grid, 2020: Introduction to energy system flexibility. Accessed 6 August 2024, <https://www.nationalgrideso.com/document/189851/download>.
- National Grid, 2023a: FES 2023 data workbook. Accessed 3 August 2024, <https://www.nationalgrideso.com/future-energy/future-energy-scenarios-fes/fes-documents>.
- National Grid, 2023b: Future energy scenarios. Tech. rep., 1–224 pp. <https://www.nationalgrideso.com/document/283101/download>.
- National Grid, 2024: Future energy scenarios: ESO pathways to net zero. Tech. rep. <https://www.nationalgrideso.com/document/322316/download>.
- NOAA CSL Chemistry & Climate Processes, 2024: Table of major mid-winter SSWs in reanalyses products. Accessed 31 July 2024, <https://csl.noaa.gov/groups/csl8/sswcompendium/majorevents.html>.
- Pearce, O., 2024: Taking the market's temperature: European hydrogen bank awards €720 million. Ammonia Energy Association, Accessed 6 August 2024, <https://ammoniaenergy.org/articles/taking-the-markets-temperature-european-hydrogen-bank-awards-e720-million/#:~:text=The%20European%20Hydrogen%20Bank%20has,renewable%20hydrogen%20over%20ten%20years>.
- Potisomporn, P., T. A. Adcock, and C. R. Vogel, 2023: Evaluating ERA5 reanalysis predictions of low wind speed events around the UK. *Energy Reports*, **10**, 4781–4790, <https://doi.org/10.1016/j.egyr.2023.11.035>, <https://www.sciencedirect.com/science/article/pii/S2352484723015603>.
- Roberts, S., 2008: Demographics, energy and our homes. *Energy Policy*, **36** (12), 4630–4632, <https://doi.org/10.1016/j.enpol.2008.09.064>.
- Scafidi, J., M. Wilkinson, S. M. V. Gilfillan, N. Heinemann, and R. S. Haszeldine, 2021: A quantitative assessment of the hydrogen storage capacity of the UK continental shelf. *International Journal of Hydrogen Energy*, **46** (12), 8629–8639, <https://doi.org/10.1016/j.ijhydene.2020.12.106>.

- Science and Technology Committee, House of Lords, 2023: Long-duration energy storage: Get on with it. Tech. rep., 1-71 pp. <https://publications.parliament.uk/pa/ld5804/ldselect/ldsctech/68/68.pdf>.
- Storage Working Group, 2022: Hydrogen storage: Delivering on the UK's energy needs. Tech. rep., 1-25 pp. https://hydrogen-uk.org/wp-content/uploads/2022/12/HUK_Hydrogen-Storage-Delivering-on-the-UKs-Energy-Needs_online.pdf.
- Storengy, 2024: Launch of the FrHyGe project, an underground hydrogen storage demonstrator. Accessed 6 August 2024, <https://www.storengy.com/en/medias/news/launch-frhyge-project-underground-hydrogen-storage-demonstrator>.
- The Royal Society, 2023a: Large-scale electricity storage. Tech. rep., 1-100 pp. <https://royalsociety.org/-/media/policy/projects/large-scale-electricity-storage/large-scale-electricity-storage-report.pdf>.
- The Royal Society, 2023b: Supplementary information to the Royal Society report on large-scale electricity storage. Tech. rep., 1-203 pp. This is not a Royal Society publication. <https://royalsociety.org/-/media/policy/projects/large-scale-electricity-storage/large-scale-electricity-storage-report---supplementary-information.pdf>.
- Van Der Most, L., K. Van Der Wiel, R. M. J. Benders, P. W. Gerbens-Leenes, P. Kerkmans, and R. Bintanja, 2022: Extreme events in the European renewable power system: Validation of a modeling framework to estimate renewable electricity production and demand from meteorological data. *Renewable and Sustainable Energy Reviews*, **170**, 1–14, <https://doi.org/10.1016/j.rser.2022.112987>.
- van der Wiel, K., H. C. Bloomfield, R. W. Lee, L. P. Stoop, R. Blackport, J. A. Screen, and F. M. Selten, 2019: The influence of weather regimes on European renewable energy production and demand. *Environmental Research Letters*, **14** (9), 2–11, <https://doi.org/10.1088/1748-9326/ab38d3>.
- Vautard, R., J. Cattiaux, P. Yiou, J.-N. Thépaut, and P. Ciais, 2010: Northern hemisphere atmospheric stilling partly attributed to an increase in surface roughness. *Nature geoscience*, **3** (11), 756–761, <http://dx.doi.org/10.1038/ngeo979>.
- Wohland, J., M. Reyers, J. Weber, and D. Witthaut, 2017: More homogeneous wind conditions under strong climate change decrease the potential for inter-state balancing of electricity in Europe. *Earth System Dynamics*, **8** (4), 1047–1060, <https://doi.org/10.5194/esd-8-1047-2017>.
- Zeng, Z., and Coauthors, 2019: A reversal in global terrestrial stilling and its implications for wind energy production. *Nature Climate Change*, **9** (12), 979–985, <https://doi.org/10.1038/s41558-019-0622-6>.
- Zhou, C., C. Azorin-Molina, E. Engström, L. Minola, L. Wern, S. Hellström, J. Lönn, and D. Chen, 2022: HomogWS-se: a century-long homogenized dataset of near-surface wind speed observations since 1925 rescued in Sweden. *Earth System Science Data*, **14** (5), 2167–2177, <https://doi.org/10.5194/essd-14-2167-2022>.